

Silicon photo-multipliers as readout for the CEDAR Cerenkov counter of the NA62 experiment at CERN

G.Collazuol, Scuola Normale Superiore and INFN Pisa
on behalf of the NA62 collaboration and
A.DelGuerra, University of Pisa
C.Plemonte, FBK-IRST
F.Sergiampietri, UCLA and INFN Pisa

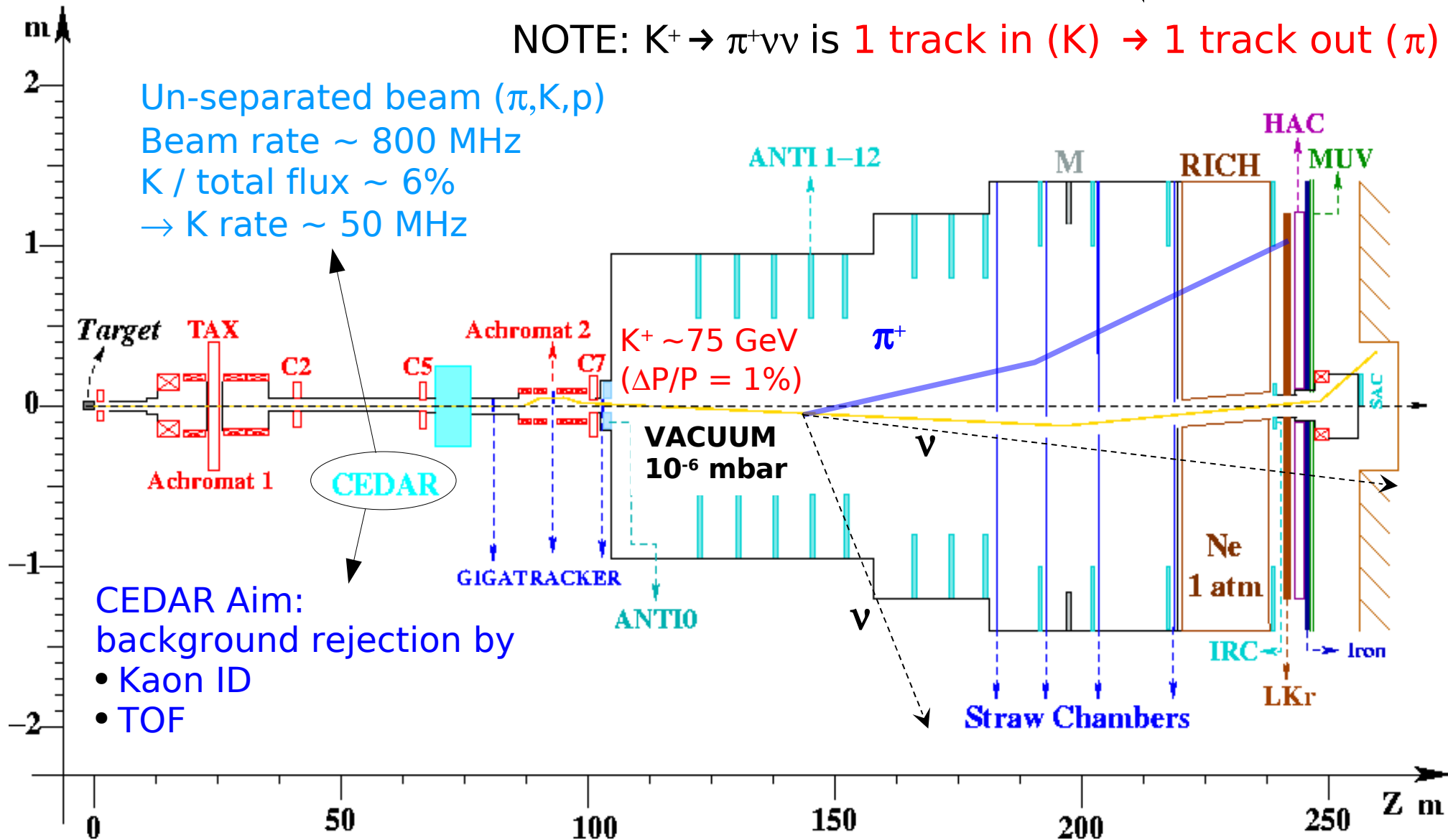
Overview

- Introduction to the $K \rightarrow \pi^+ \nu \bar{\nu}$ experiment NA62
- The CEDAR detector for tagging Kaons in a high intensity beam
- Summary of the SiPM physics and performances
- SiPM as read-out for the CEDAR counter
- Conclusions

Experiment NA62 (Proposal P326) at CERN

Goal: to measure $O(100)$ ultra rare decays $K^+ \rightarrow \pi^+ \nu \bar{\nu}$ at the CERN SPS
 Experimental method: K decay in flight in vacuum
 Beam: High energy, monochromatic, high intensity

NOTE: $K^+ \rightarrow \pi^+ \nu \bar{\nu}$ is 1 track in (K) \rightarrow 1 track out (π)



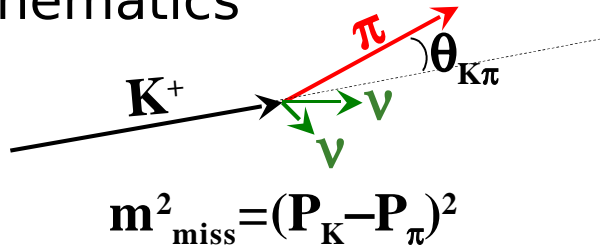
Experiment NA62 (Proposal P326) at CERN

Signal: $O(100)$ $K^+ \rightarrow \pi^+ \nu \nu$ events

- $BR(SM) = 8 \times 10^{-11}$
 - Signal acceptance 10%
 - K decays $\sim 10^{13}$
-
- Kaon decay in flight technique
 - Intense proton beam from SPS
 - High energy K ($P_K = 75$ GeV/c)
 - Tracking all beam particles
 - Tagging Kaons with a Cerenkov counter

Low Level of background (S/N < 10%) & Redundancy

- Kinematics



- Vetoes

- Redundant Particle ID

-
- Kaon: Beam Tracker (Silicon pixels)
 - Pion: Spectrometer (Straws tubes)
-
- Small angle charged & neutral vetoes
 - NA48 liquid Krypton calorimeter (mid. θ)
 - Large angle calorimeter rings as anti's
 - Spectrometer for charged trks. rejection
-
- Calorimeter (NA48 LKr) for γ/μ detection
 - RICH for π/μ separation + TOF
 - CEDAR for K identification + TOF
 - Muon filter

The CEDAR detector at CERN

CErenkov Differential counter with Achromatic Ring focus (CEDAR)

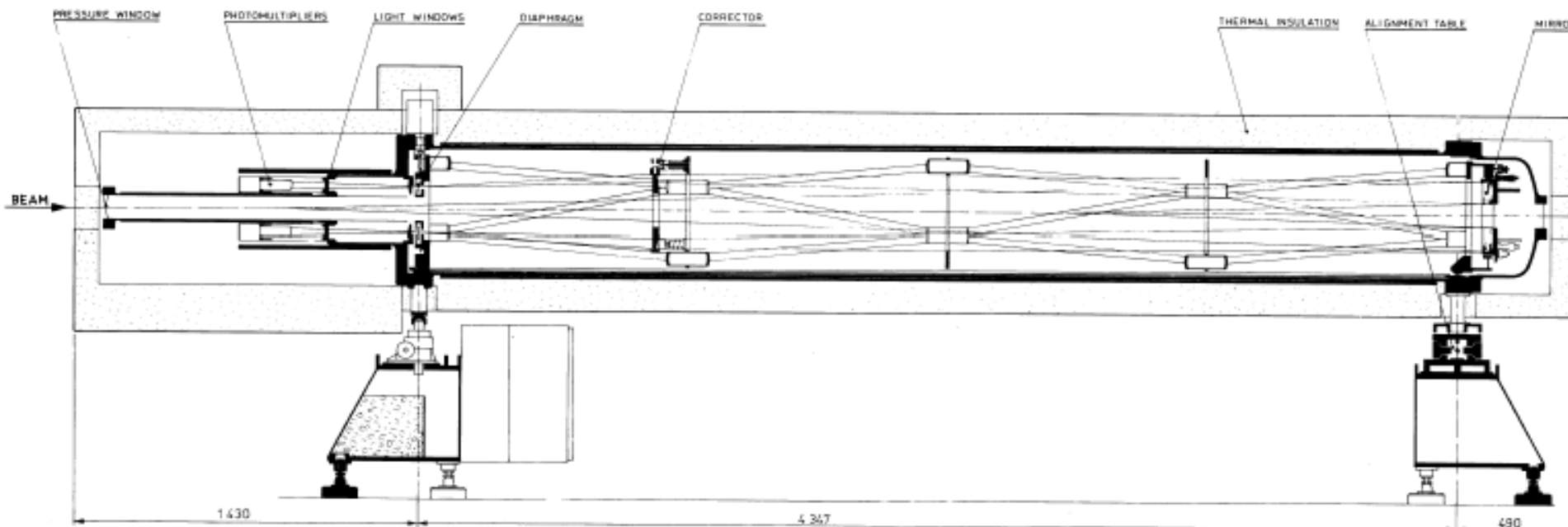
The CEDAR is used at CERN since 70-ies for the identification and selection of particles in the secondary beams of the SPS. By tuning gas pressure and diaphragm aperture it can separate kaons from pions up to 300 GeV/c and detect protons down to 60 GeV/c.

In NA62 the CEDAR counter will be crucial for:

- tagging K in order to **reject background events due to beam (π , p) interactions** with residual gas by TOF: w/o CEDAR the required vacuum level $P \sim 10^{-6}$ mbar would be $P \sim 10^{-7}$ mbar \rightarrow **huge impact in vacuum system cost**
- **rejecting accidental hits in the beam tracker**
- **trigger purposes and beam geometry/intensity on-line monitoring**

APPENDIX C

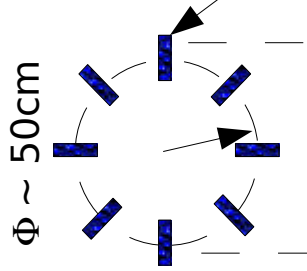
GENERAL MECHANICAL DRAWING



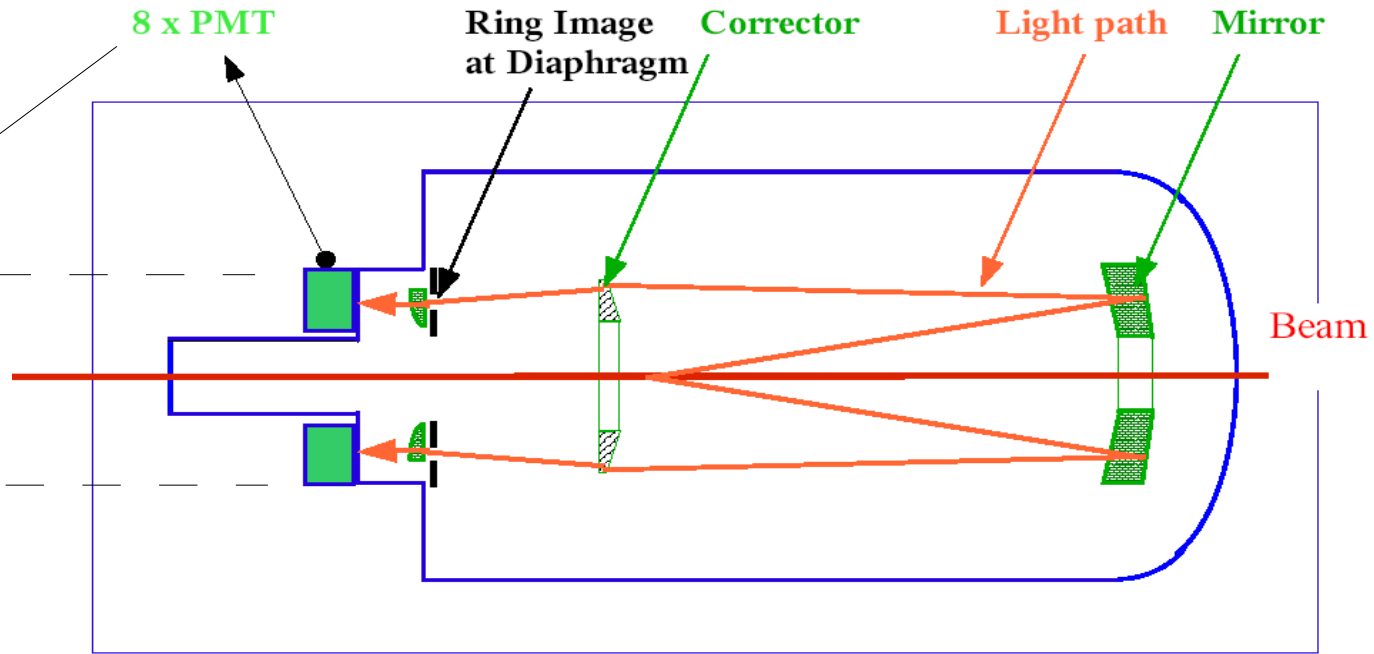
Bovet, Maleyran, Piemontese, Placci, Placidi CERN yellow report 82-13 (1982)

The CEDAR detector at CERN

Current optics condenses the cerenkov light from the diaphragm into 8 light spots ($\sim 1 \times 3 \text{ cm}^2$ each)



Cerenkov light yield:
 ~ 100 photons per Kaon



NA62 requirements:

Minimal material budget: use H_2 (2.6 bar)

Kaon tag efficiency $> 95\%$

Contamination $< 10^{-6}$

Pion rate $\sim 800 \text{ MHz}$

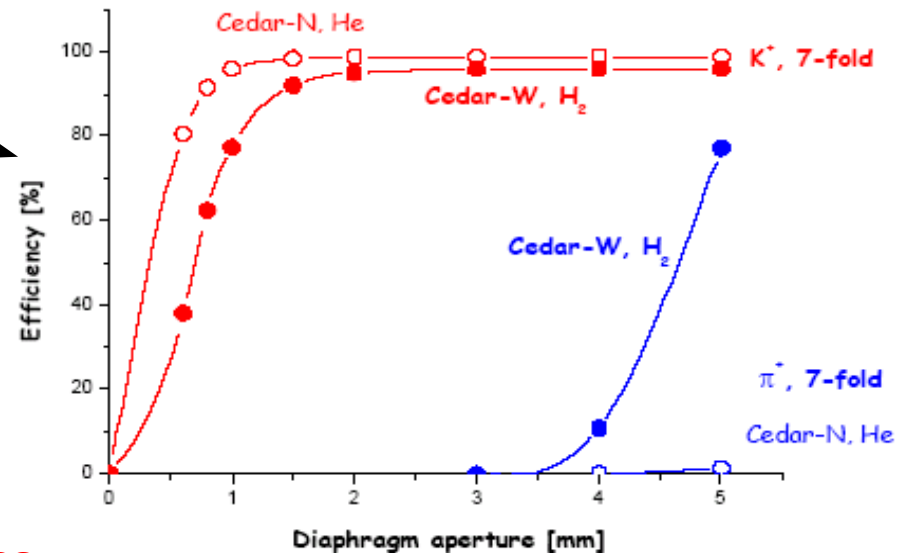
Kaon rate $\sim 50 \text{ MHz}$

\rightarrow photon rate $\sim 2 \text{ MHz} / \text{mm}^2$

$\sim \times 10$ the limit of the old readout

Need new read-out detector and electronics

Cedar N(He) versus W(H₂) Comparison



Calculations by L.Gatignon

Study for a CEDAR readout with SiPM's

Key points for the new detector:

- **Single photon counting** application
- Stand **very high photon rate / unit area** (occupancy in time and space)
- The **smaller the active area** the better (beam activity)
(minimum $\sim 12 \text{ cm}^2$ due to optics phase space)
- **UV/Blue light sensitivity** with the highest efficiency (PDE)
- Excellent **timing resolution** on single photon
- Exposition to the halo of intense hadron beam (**radiation damages**)

Do SiPM provide a valid alternative to PMT ?

- very good **rate capabilities** and granularity
- excellent **efficiency** and **timing resolution** for single photons
- **cheaper than PMT's** (cost of the readout \sim photon rate / unit surface)

→ **Worth investigating on it**

Which devices ?

Today many institutes/companies are involved in SiPM development/production:

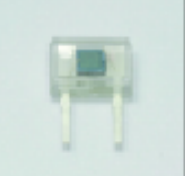


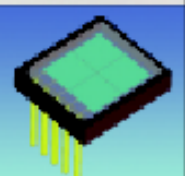
- Hamamatsu (HPK), Hamamatsu City, Japan
- FBK-IRST, Trento, Italy → collaboration with INFN (“MEMS” project)
(formerly ITC-IRST)
- SensL, Blackrock, Ireland
- MPI, Munich, Germany
- Zecotek, Vancouver, Canada
- RMD, Boston, USA
- JINR/Micron Enterprise, Dubna and Zelenograd, Russia
- MePhi/Pulsar Enterprise, Moscow, Russia
- Center of Perspective Technology and Apparatus (CPTA), Moscow /
Photonique, Geneve, Switzerland

→ Our studies based mainly on HPK and IRST devices

Recent products from Hamamatsu

Preliminary Future MPPC designs

HAMAMATSU has been developing and producing a variety of MPPC devices to make them even easier to use and more beneficial in more applications.

Type	Image	Effective active area	Number of pixels	Pixel size (μm)	Package	
Plastic type		1 x 1 mm	1600	25 x 25	Plastic	
Ceramic type		1.3 x 1.3 mm	657	50 x 50	Ceramic	
			165	100 x 100		
Surface mount type		1 x 1 mm	1600	25 x 25	Plastic	
			400	50 x 50		
			100	100 x 100		
Large active area	Surface mount type	3 x 3 mm	14400	25 x 25	Plastic	
			3600	50 x 50		
			900	100 x 100		
	Array type		6 x 6 mm (2 x 2 array)	14400/element	25 x 25	Ceramic
				3600/element	50 x 50	
				900/element	100 x 100	

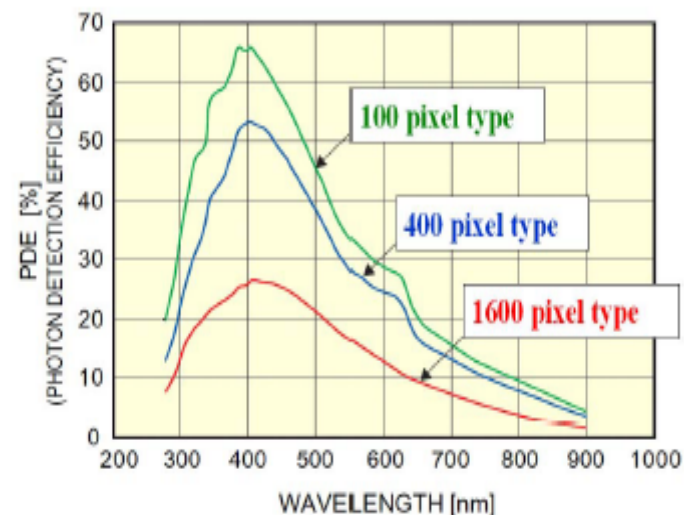


Fig.3 PDE vs. wavelength

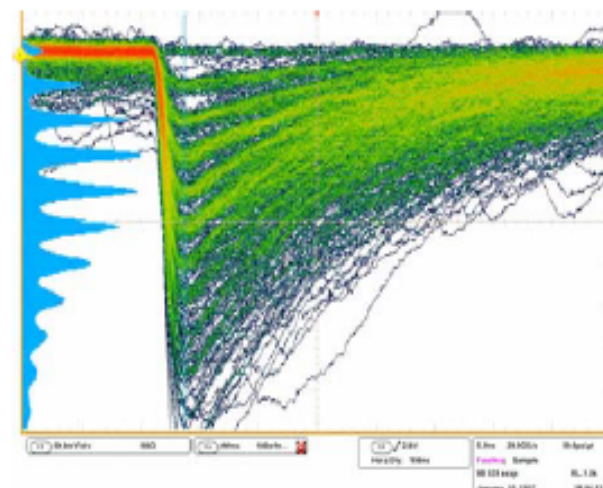
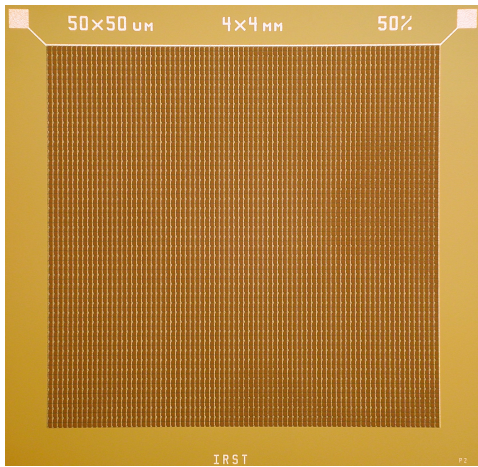


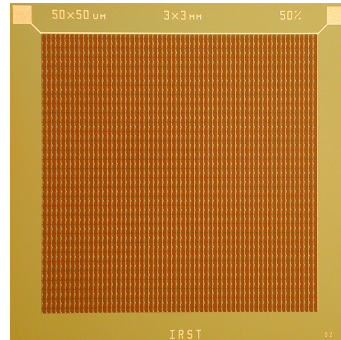
Fig.9 The output pulse of 3 x 3 mm MPPC at 25 degree

Recent production at FBK-IRST

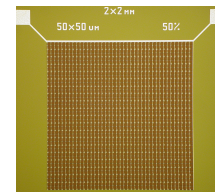
4x4 mm²
6400 cells



3x3 mm²
3600 cells

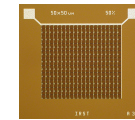


Cell size	Fill factor (fraction of active surface)
40 x 40 μm ²	44%
50 x 50 μm ²	50%
100 x 100 μm ²	76%

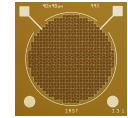


2x2 mm²
1600 cells

pad: 1x1 mm²

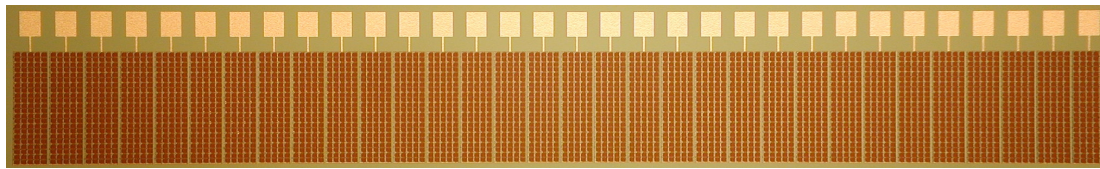


1x1 mm²
400 cells

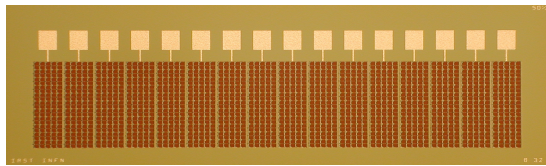


circular

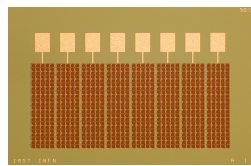
Array 32x



Array 16x

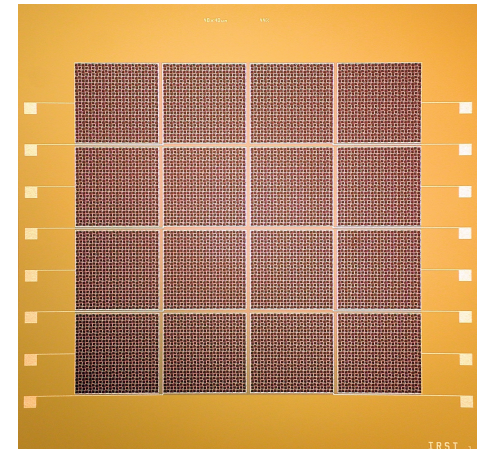


Array 8x



pad: 1.1 x 0.25 mm²

Matrix 4x4





Short summary of SiPM physics and performances

More detail at
http://collazug.home.cern.ch/collazug/seminario_sipm_fe.pdf

The building block of a SiPM: GM-APD cell

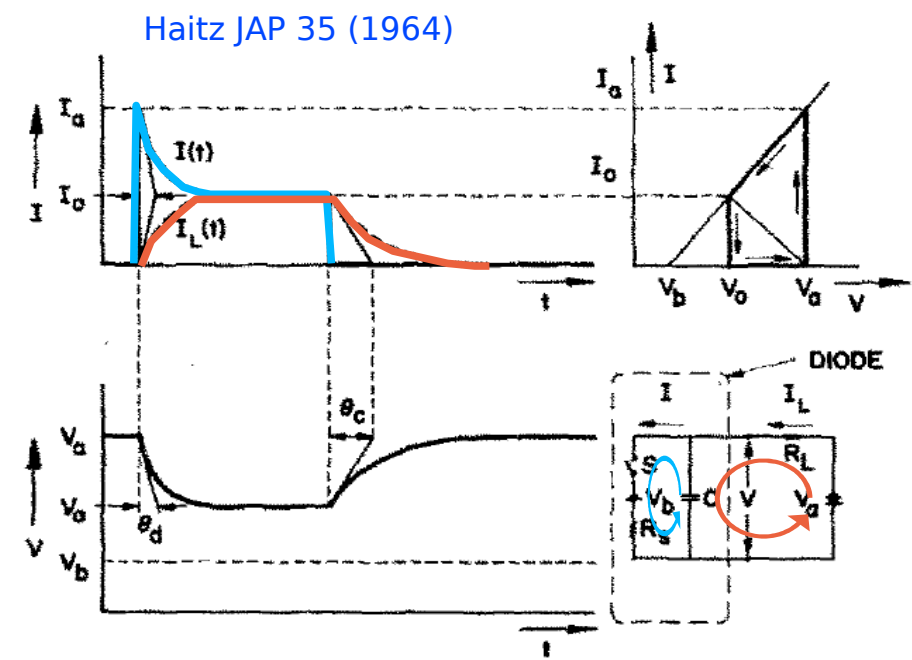
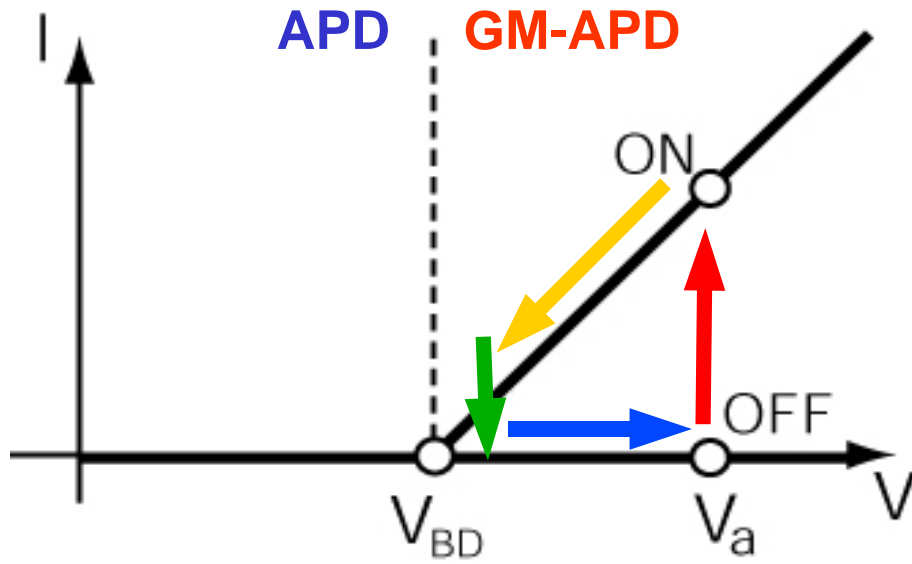
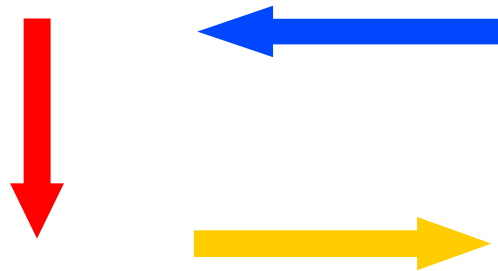


FIG. 3. Shape of current pulse for $\theta_d \ll \tau_{r1}(I_0)$.

OFF condition: avalanche quenched, switch open, capacitance charged until no current flowing from V_{BD} to V_{BIAS} with time constant $R_q \times C_D = \tau_{Quenching}$ (\rightarrow recovery time)

P_{01} = turn-on probability
probability that a carrier traversing the high-field region triggers the avalanche

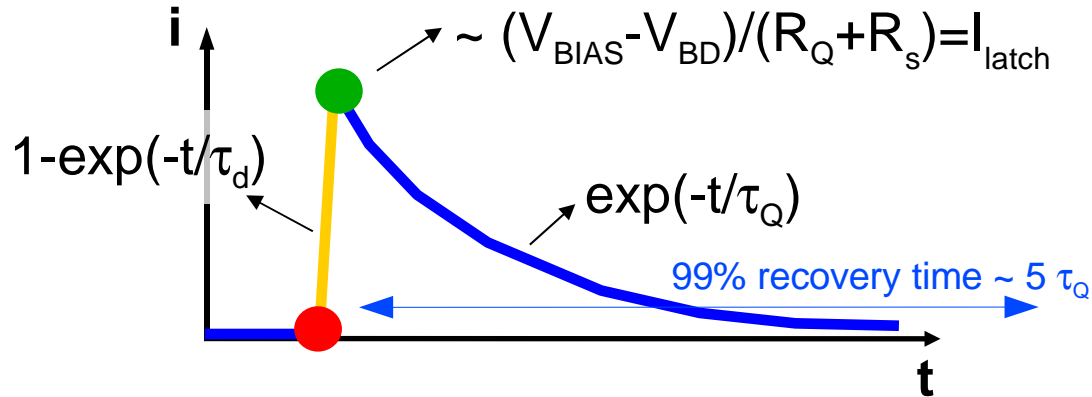


P_{10} = turn-off probability
probability that the number of carriers traversing the high-field region fluctuates to 0

ON condition: avalanche triggered, switch closed
 C_D discharges to V_{BD} with a time constant $R_s \times C_D = \tau_{discharge}$,
at the same time the external current asymptotic grows to $(V_{BIAS} - V_{BD}) / (R_Q + R_s)$

Operation principle of a GM-APD cell

If R_Q is high enough the internal current is so low that statistical fluctuations may quench the avalanche



The leading edge of the signal is much faster than trailing edge:

1. $\tau_d = R_S \cdot C_D \ll R_Q \cdot C_D = \tau_Q$
2. turn-off mean time is very short
(if R_Q is sufficiently high, $I_{latch} \sim 10\mu A$)

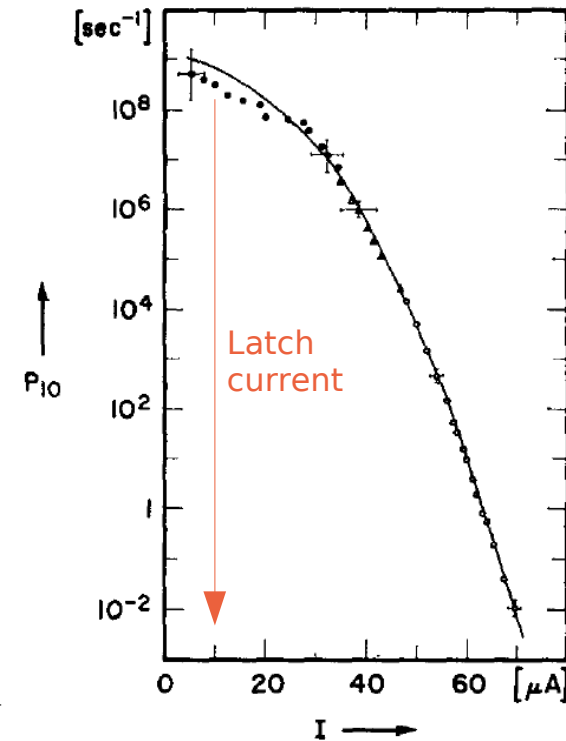


FIG. 2. Turnoff probability per second as function of pulse current.
Haitz JAP 35 (1964)

The charge collected per event is the area under the exponential which is determined by circuital elements and bias.

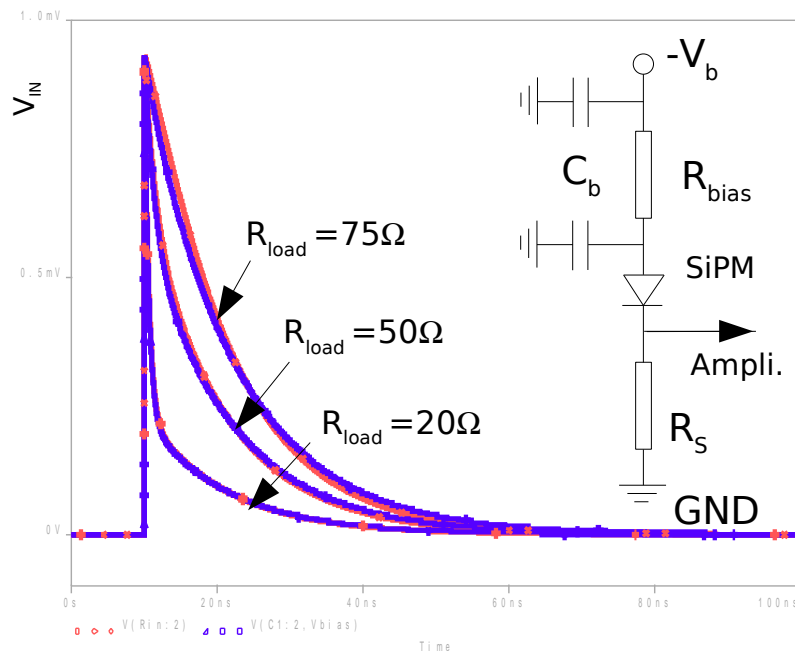
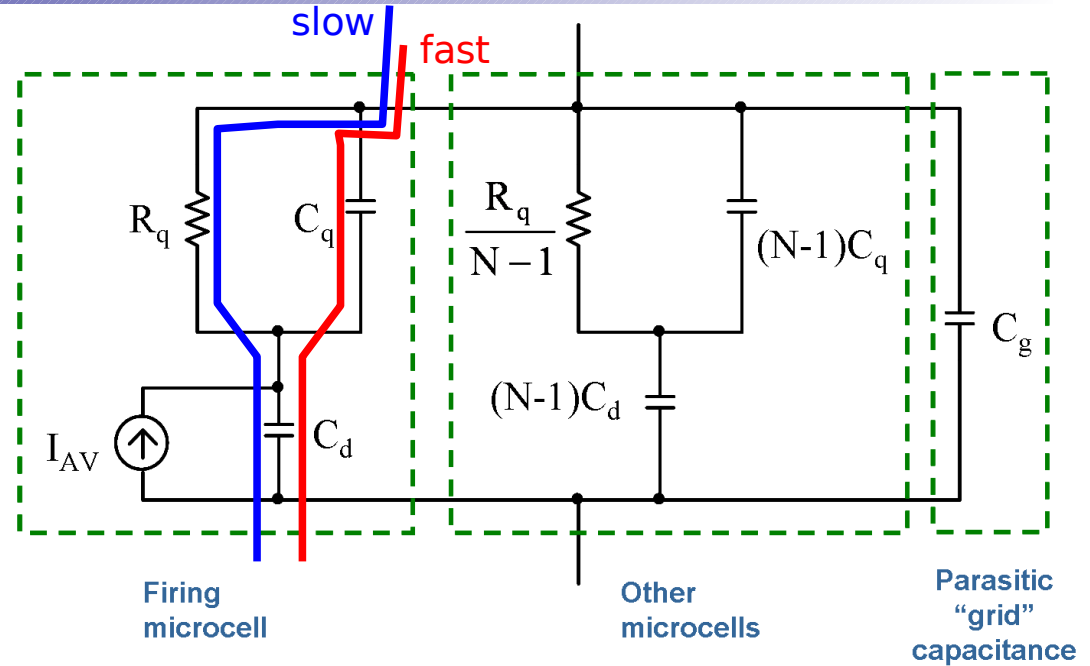
➡ It is possible to define a GAIN (discharge of a capacitor !!!)

$$G = \frac{I_{max} \cdot \tau_Q}{q_e} = \frac{(V_{bias} - V_{BD}) \cdot \tau_Q}{(R_Q + R_S) \cdot q_e} = \frac{(V_{bias} - V_{BD}) \cdot C_D}{q_e}$$

The gain fluctuation in GM-APD is very small (\ll than for APD)

Electrical model of a SiPM

- R_q : quenching resistor (hundreds of $k\Omega$)
- C_d : junction capacitance (few tens of fF)
- C_q : parasitic capacitance in parallel to R_q (few tens of fF, $C_q < C_d$)
- I_{AV} : SiPM ~ ideal current source current source modeling the total charge delivered by a cell during the avalanche $Q = \Delta V(C_d + C_q)$
- C_g : parasitic capacitance due to the routing of V_{bias} to the cells (metal grid, few tens of pF)



1) the peak of V_{IN} is independent of R_s

A constant fraction Q_{IN} of the charge Q delivered during the avalanche is instantly collected on $C_{tot} = C_g + C_{eq}$.

2) The circuit has two time constants:

- $\tau_{IN} = R_s C_{tot}$ (fast)
- $\tau_r = R_q (C_d + C_q)$ (slow)

Decreasing R_s , the time constant τ_{IN} decreases, the current on R_s increases and the collection of Q is faster

Detector performances

related to the **recharge of the diode capacitance** from V_{BD} to V_{bias} during the avalanche quenching time after I_{latch} is reached.

$$G = (V_{BIAS} - V_{BD}) * C_D / q$$

valid for few volts above V_{BD}

Gain

pulses triggered by non-photo-generated carriers (**thermal / tunneling generation** in the bulk or in the surface depleted region around the junction)

carriers can be trapped during an avalanche and then released triggering another avalanche

Noise: dark count
after-pulsing
optical cross-talk

photo-generation during the avalanche discharge. Some of the photons can be absorbed in the adjacent cell possibly triggering new discharges

$$PDE = QE * P_{01} * \epsilon$$

QE = quantum efficiency

P_{01} = avalanche triggering prob.

ϵ = geometrical fill factor

Photo-detection efficiency

Dynamic Range

Related to the density of cells and recovery time

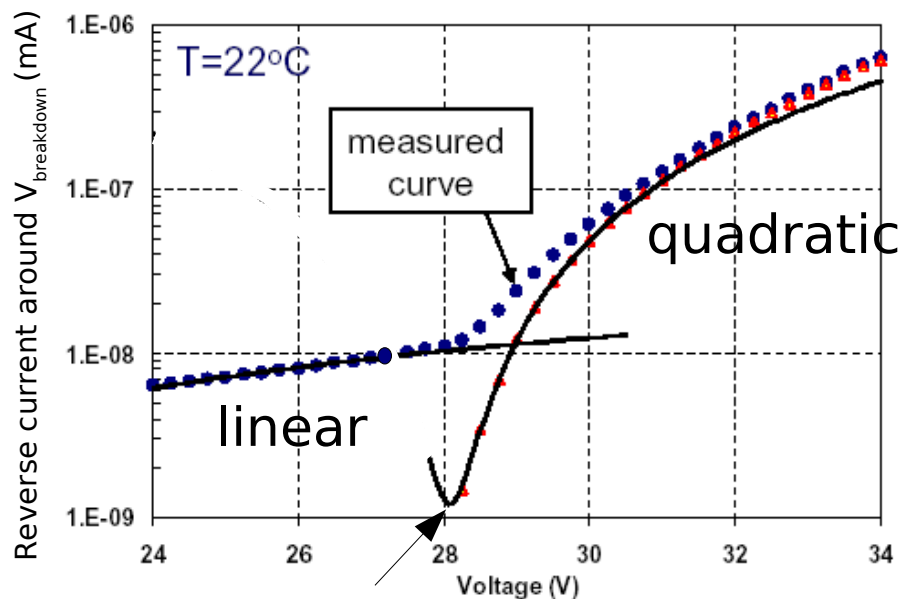
Related to the photo-generation and to the **avalanche propagation**

Time resolution

Static characteristics (I-V measurement)

First tests to verify the functionality of the device:

- Breakdown voltage (V_{bd})
- Dark count rate (N_{dark})
- Quenching resistor value R_Q

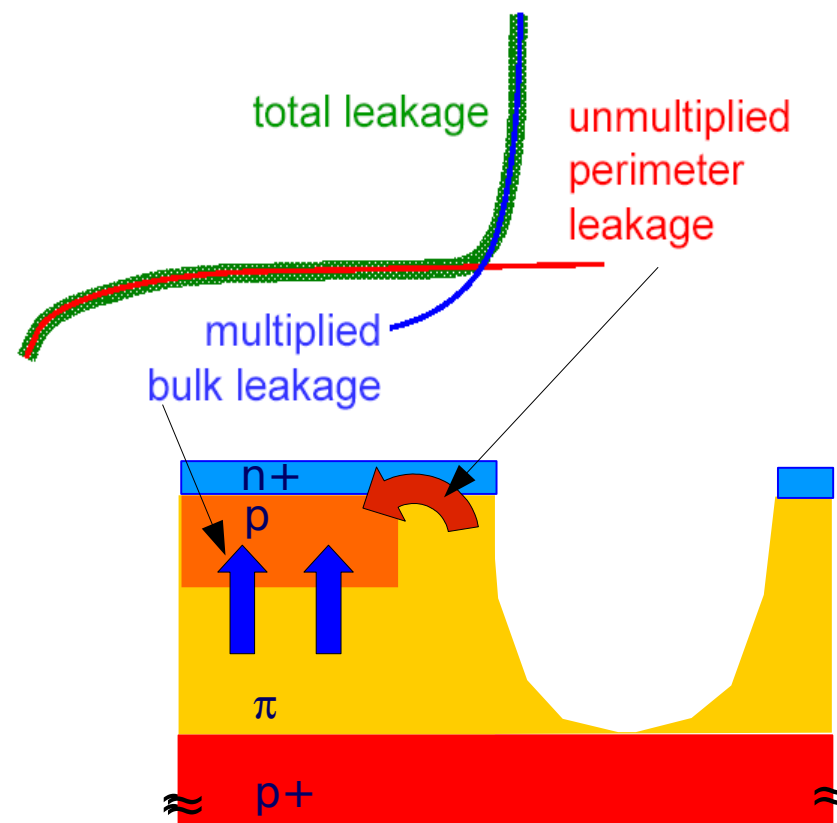


Pre-breakdown: current mainly due to generation in the surface region around diode:

$$I_{pre-BD} \sim V_{bias} \text{ (linear)}$$

Post-breakdown: up to few V current due dark events is:

$$I_{post-BD} = q \cdot G \cdot N_{dark} \sim q \cdot V_{bias} \cdot V_{bias} \text{ (quadratic)}$$

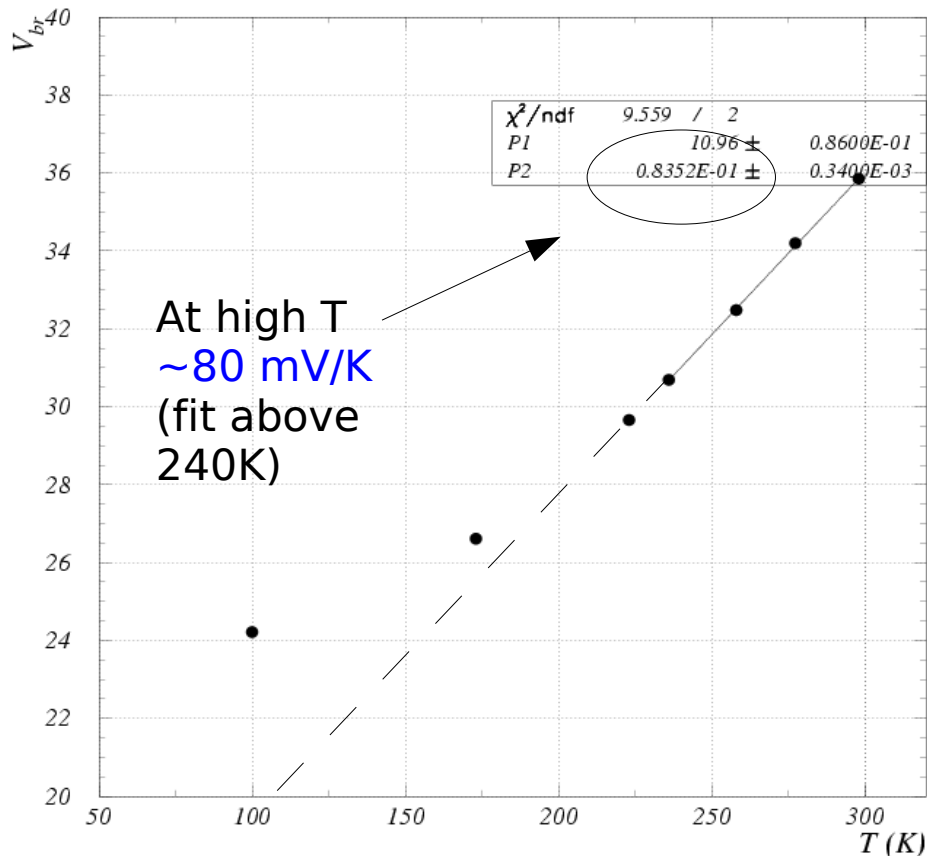


Technological issues:

- **Uniformity of layout**
check spread of V_{BD} in a wafer (typ. < 1%)
- **Uniformity of dark count rate**
check spread of post-breakdown current
- **Yield of good devices**
Fraction of devices showing anomalous current behavior (e.g. at IRST < 20%)
Due to rare defects. Crucial parameter for matrices on the same substrate.

V_{BD} Break-Down vs T

Data (IRST devices)



Baraff Model PR 128 (1962) 2507

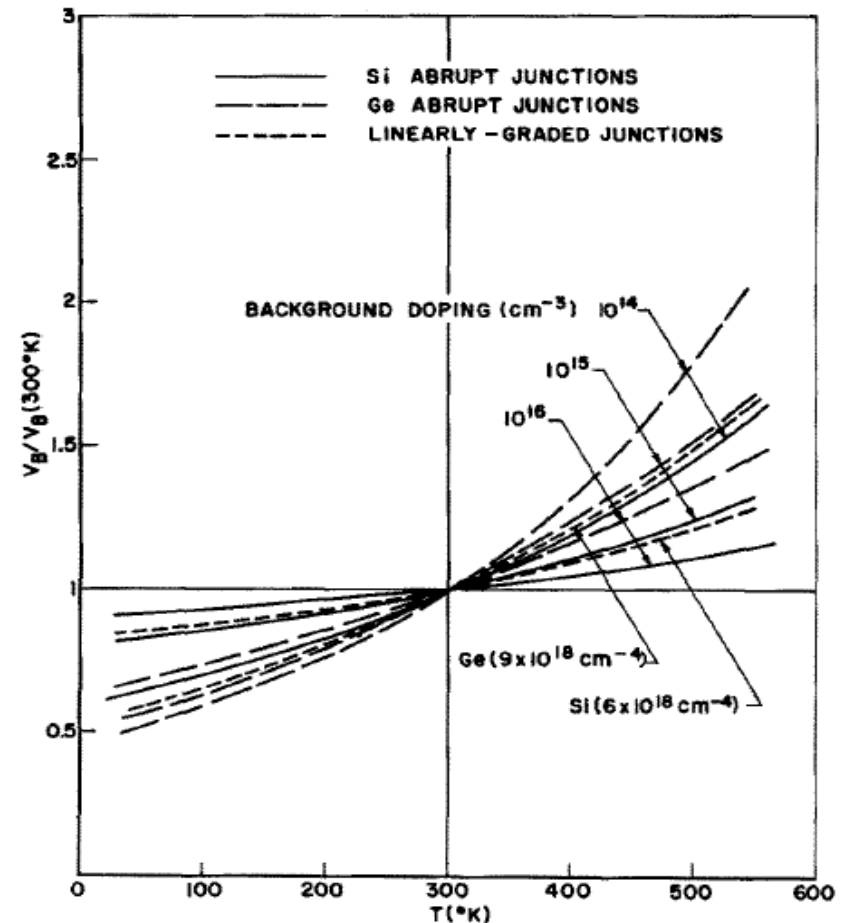


Fig. 4. Breakdown voltage vs temperature for Si and Ge p - n junctions. $V_B(300^\circ\text{K})$ is 2000, 330, and 60 V for Si and 950, 150, and 25 V for Ge for dopings of 10^{14} , 10^{15} , and 10^{16} cm^{-3} respectively. The linear-graded junctions have $V_B(300^\circ\text{K})$ the same as those for doping of 10^{15} cm^{-3} .

G.Collazuol

Acknowledgments: A.Baldini, A.Brez – INFN Pisa

Crowell and Sze, APL 9 (1966) 242

Dynamic characteristics

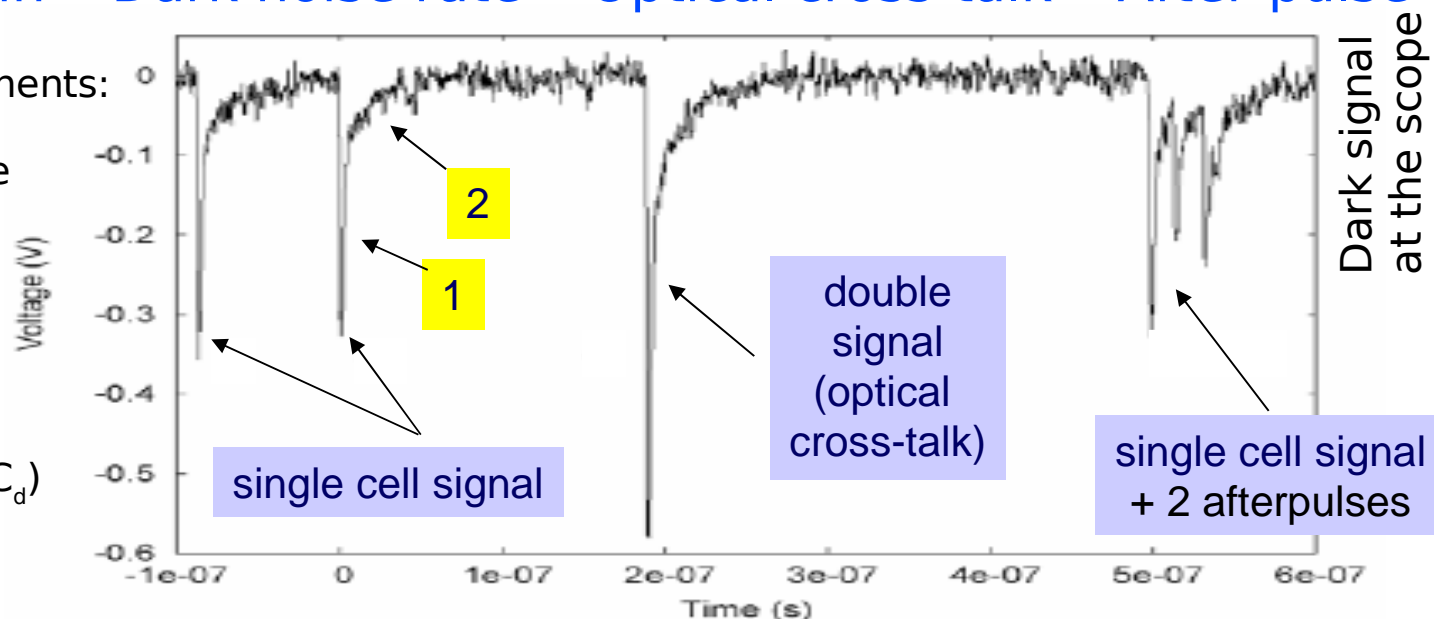
Complete characterization of signal and noise:

- Signal shape • Gain • Dark noise rate • Optical cross-talk • After-pulse

The signal presents 2 components:

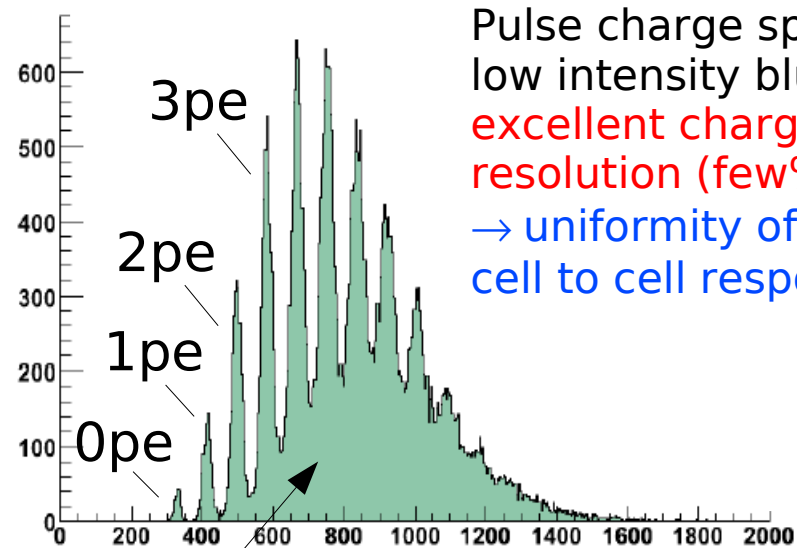
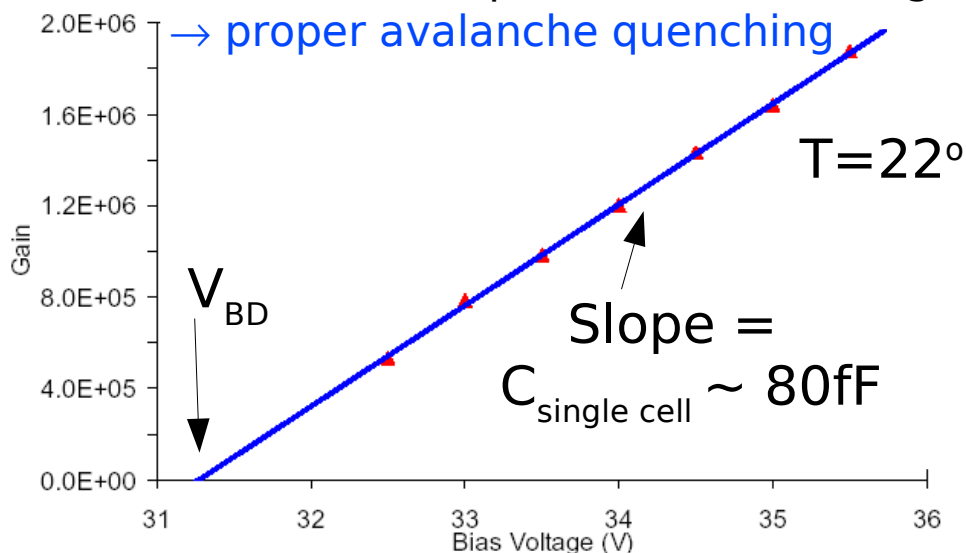
1. **fast component**: avalanche current reproduced at the output by **parasitic capacitor**

2. **slow component** due to the **recharge of the diode capacitance** (99% recovery time $\sim 100\text{ns}$, depending on C_d)



Gain is linear up to $\sim 5\text{V}$ overvoltage

\rightarrow proper avalanche quenching



Pulse charge spectrum low intensity blue LED

excellent charge resolution (few%)

\rightarrow **uniformity of cell to cell response**

NOTE: very **easy to measure the gain** (wrt PMT !!!)

(IRST devices)

T dependence: V_{BD} , τ_Q and Gain

V_{BD} breakdown voltage: V_{BD} increases with T:

At higher T carriers loose more to lattice
 → lower mobility, shorter mean free path (λ)
 → carriers need higher V to impact-ionize
 (temp. coefficient $\Delta V_{BD}/\Delta T \sim 20\text{mV/K} - 80\text{mV/K}$
 depending on doping concentration)

Recovery time: τ_Q decreases with T

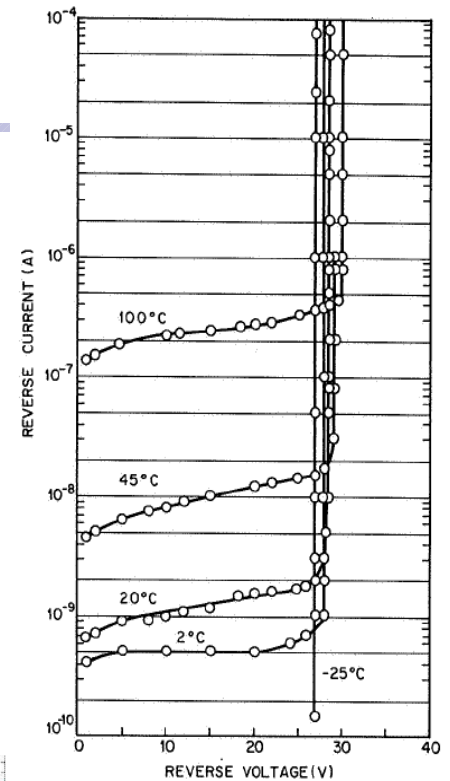
Due polysilicon R_Q properties

T (K)	R_Q (M Ω)
300	0.2
200	0.4
77	1.7

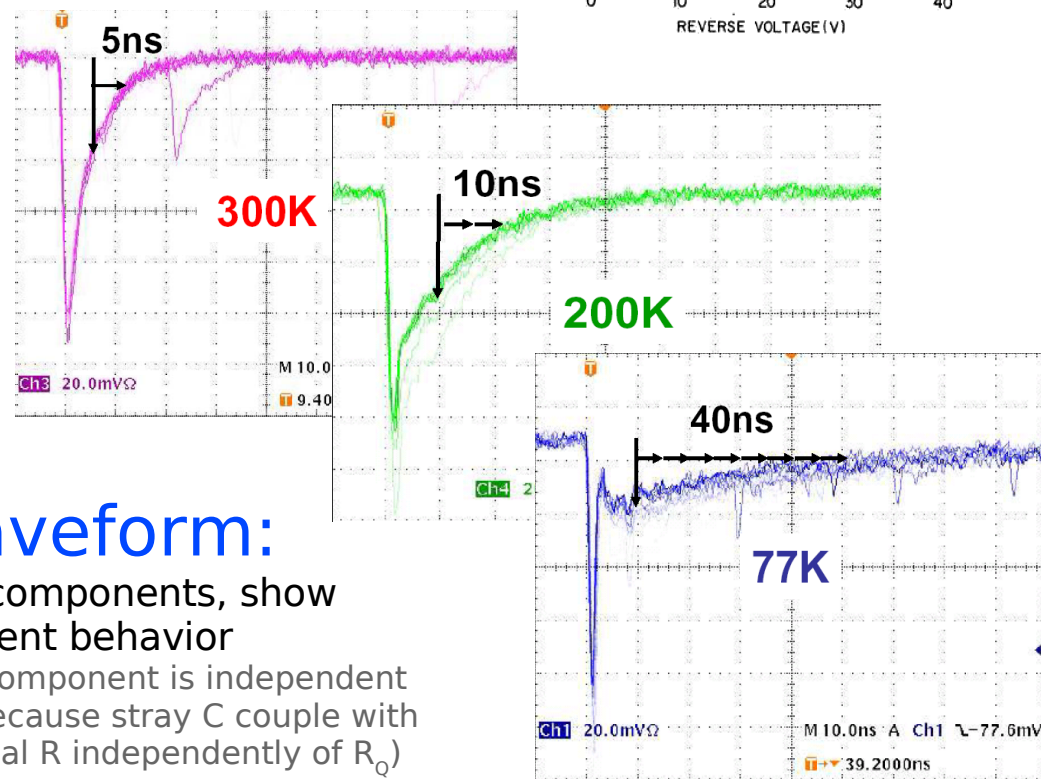
H.Otono – PD07
 Characterization
 of SiPM by HKP at low T

Cell Capacity does not vary with T

Gain independent of T
 at fixed Over-Voltage



Haitz JAP 34 (1963)



Waveform:

Two components, show
 different behavior
 (fast component is independent
 of T because stray C couple with
 external R independently of R_Q)

Photo-detection efficiency (PDE)

$$PDE = N_{\text{pulses}} / N_{\text{photons}} = QE \cdot P_{01} \cdot \epsilon_{\text{geom}}$$

Carrier Photo-generation

(QE = probability for a photon to generate a carrier that reaches the high field region)

*

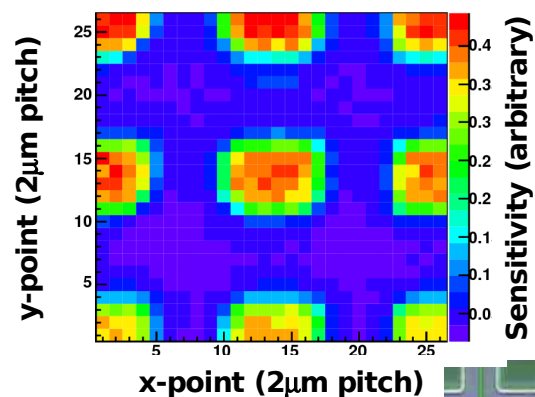
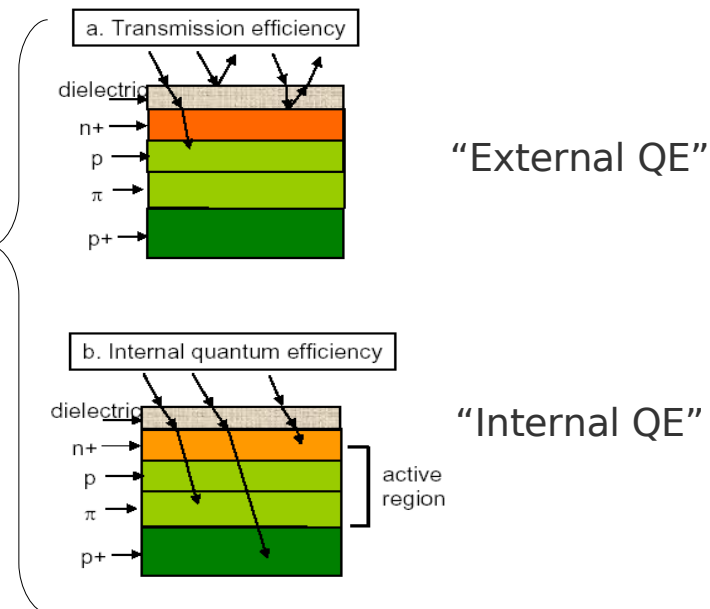
Avalanche triggering

(P_{01} = probability for a carrier traversing the high-field to generate the avalanche)

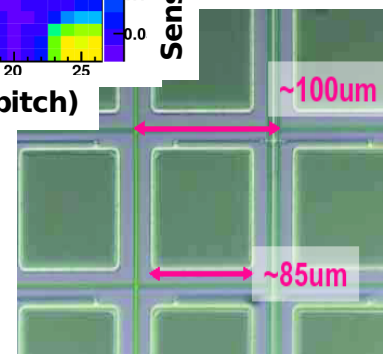
*

Geometrical fill factor

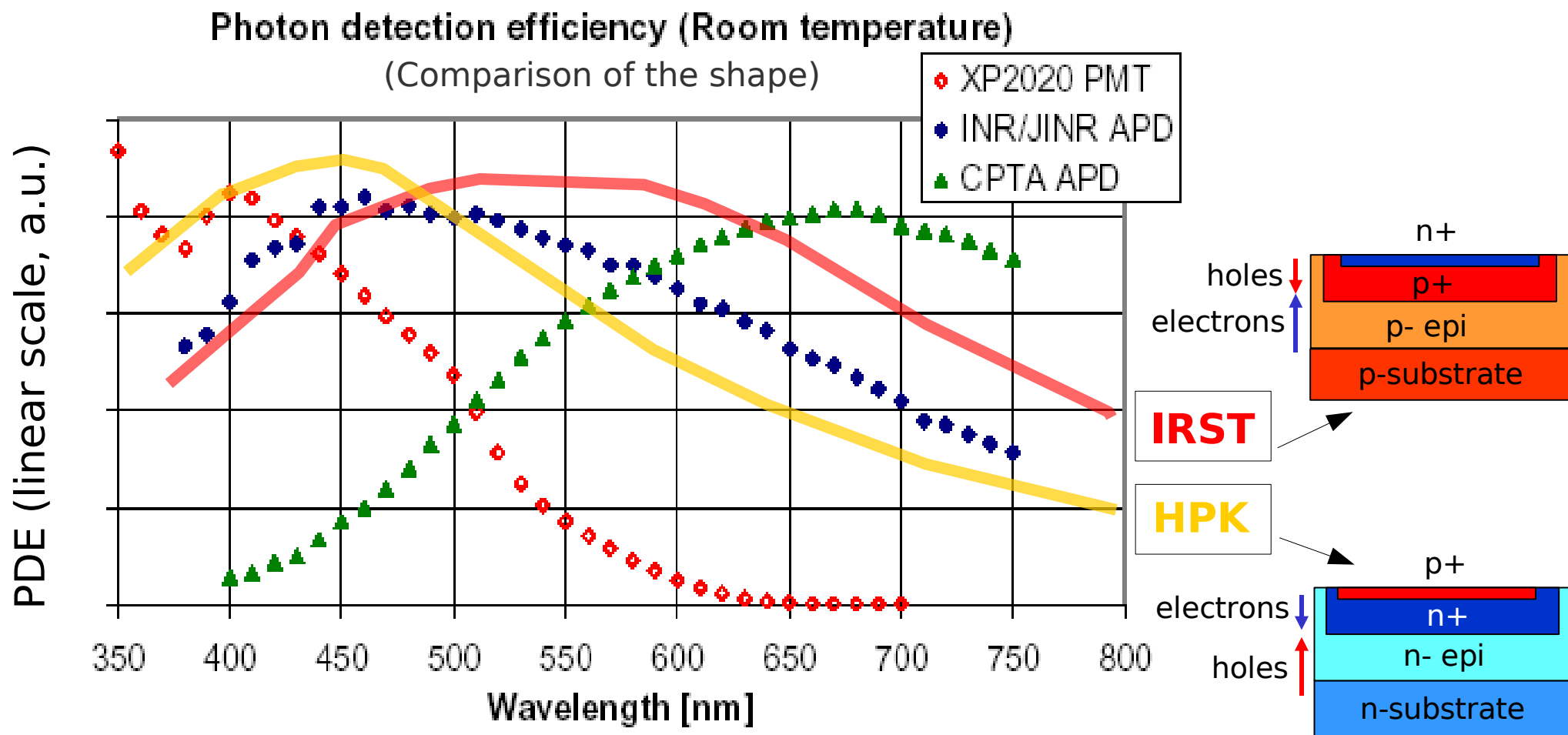
(ϵ = fraction of dead area due to structures between the cells, eg. guard rings, trenches)



Hamamatsu SiPM close up



PDE VS wavelength shape: comparison

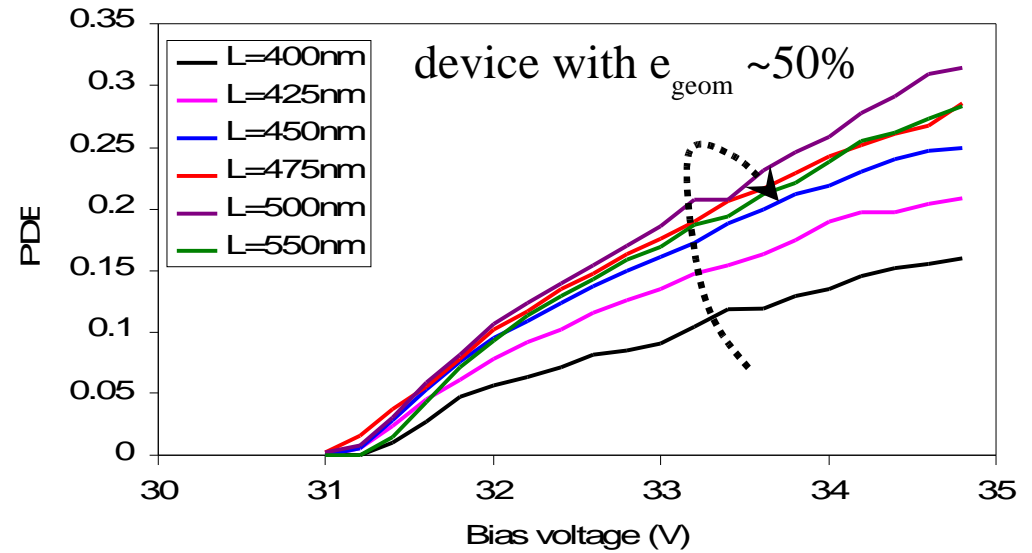


NOTE:

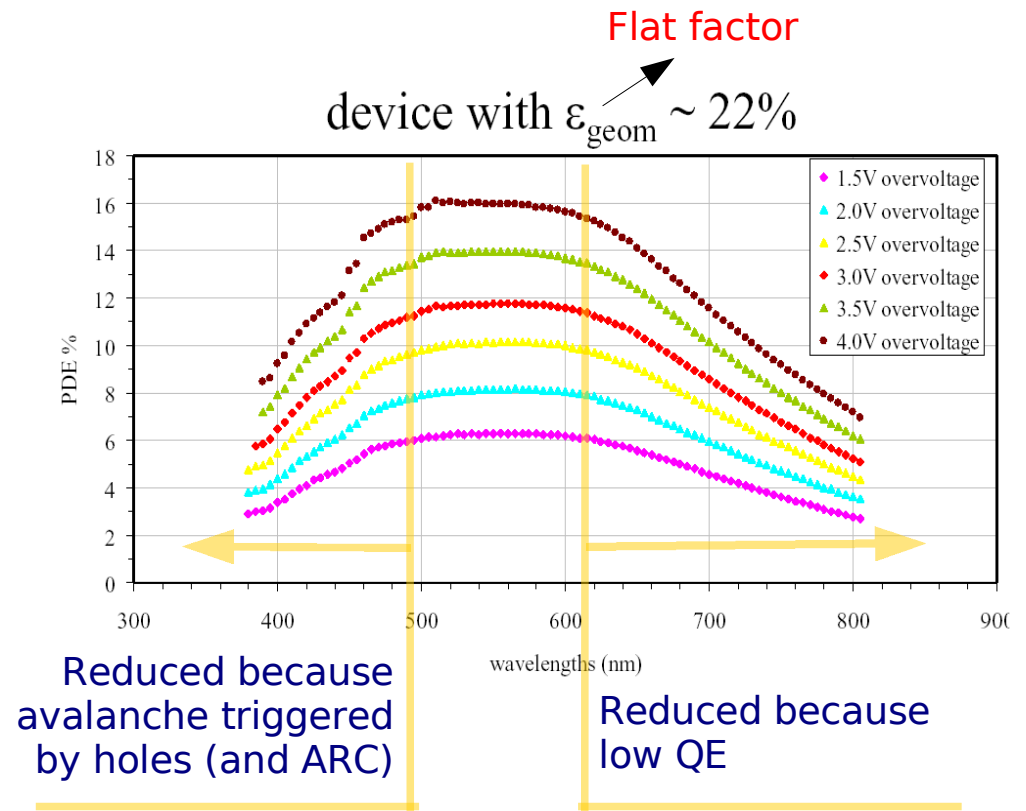
- The absolute scale (peak value) is set by fill factor (up to 70%) and over-voltage
- Obviously PDE shape is extremely dependent of the structure:
 p-on-n (where essentially electrons trigger avalanches for short wavelengths) is naturally more blue sensitive than n-on-p (holes trigger avalanches for short wavelengths)
- The use of WLS on the surface (enhance PDE to short wl) degrades the timing resolution

IRST devices – PDE vs over-voltage and λ

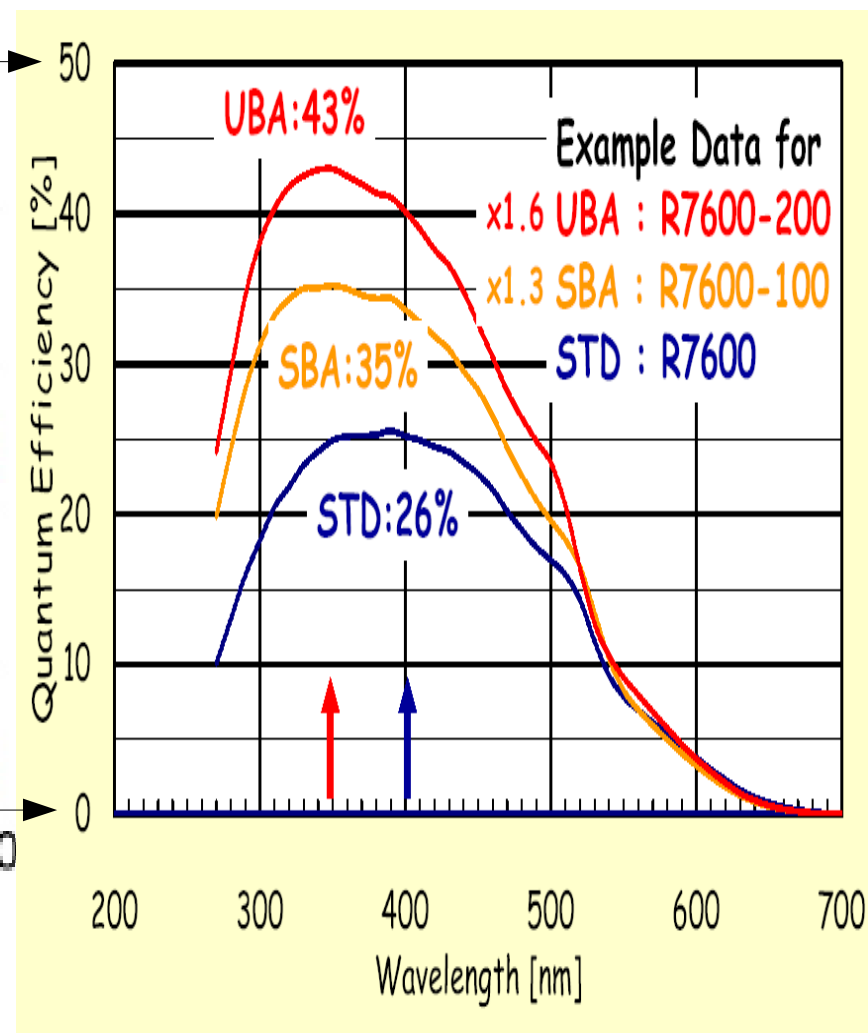
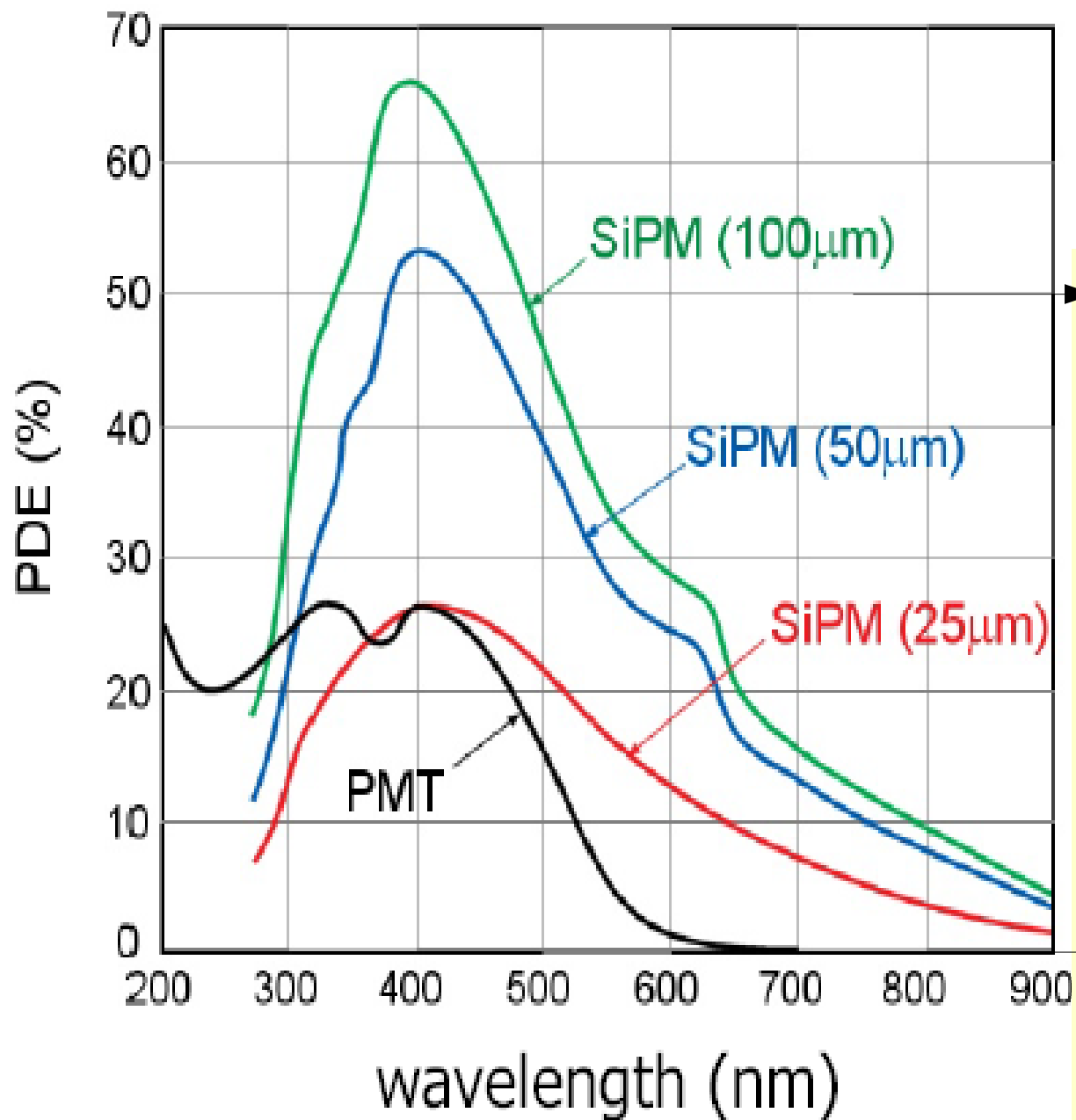
PDE
Linear dependence on ΔV



PDE
Dependence on wavelength



Hamamatsu: PDE of SiPM vs QE of PMT



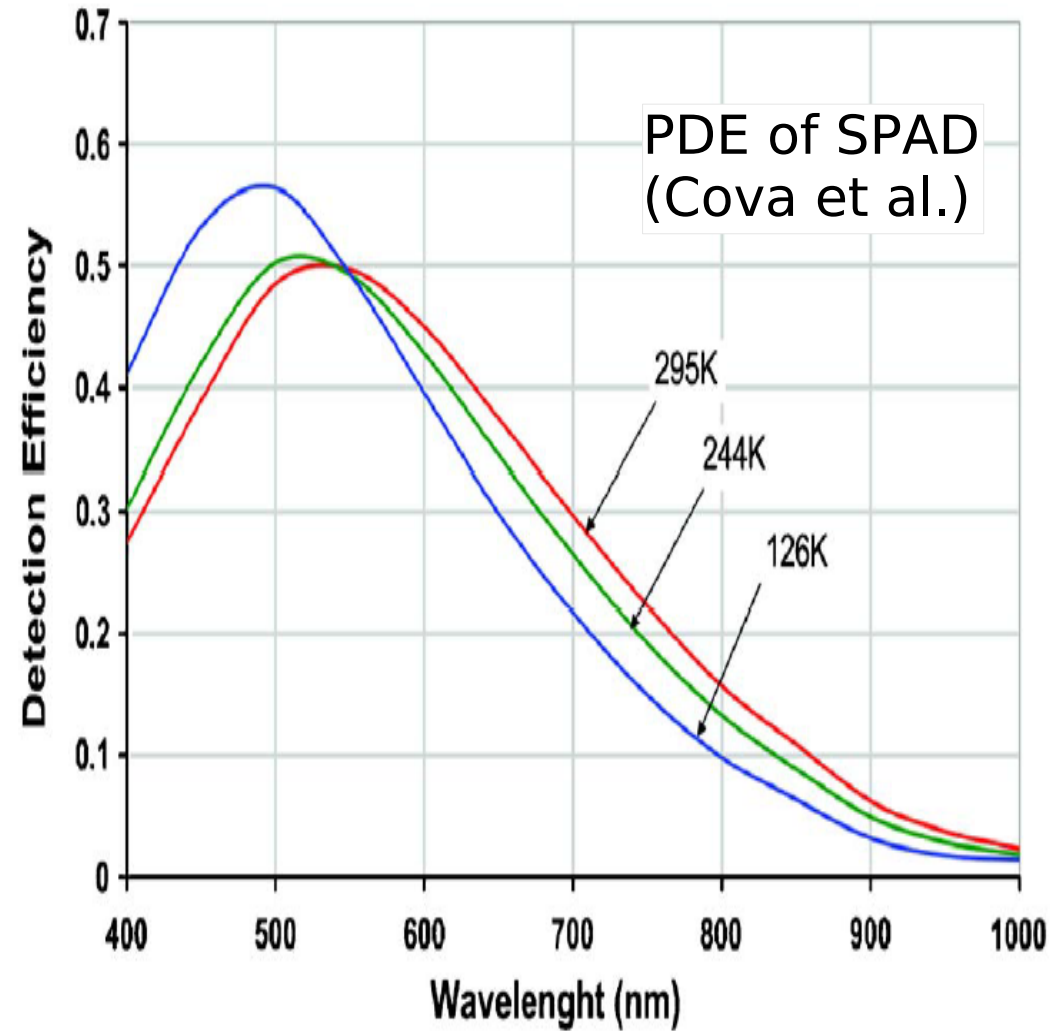
T dependence: PDE (SPAD devices)

PDE:

Combination of two effects:

1. P_{01} increases at low T (impact ioniz.)
2. Energy gap increases at low T

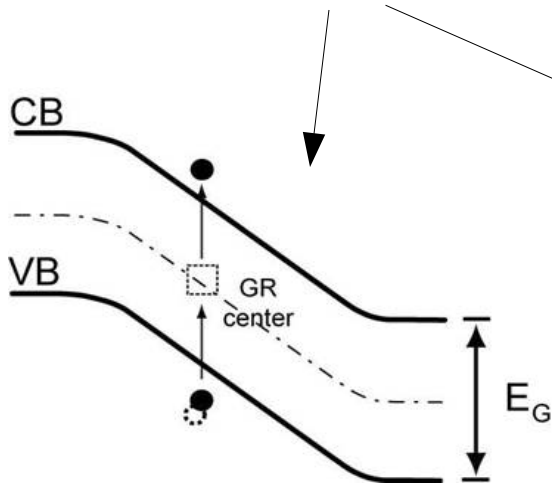
(Over-voltage fixed)



I.Rech et al, Rev.Sci.Instr. 78 (2007)

Dark count rate: free carrier generation

Main mechanisms

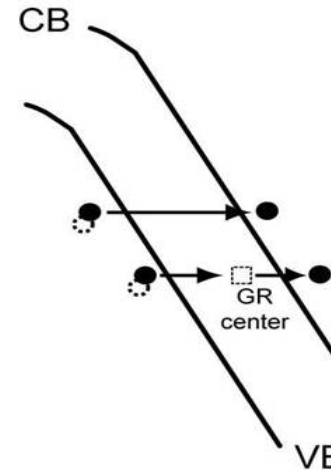


(1) Generation - Recombination Centers
SHR generation (Field Enhanced)
in the depletion region

$$\frac{dN_{\text{emiss}}}{dt} \equiv \frac{n_i}{2\tau_g}$$

n_i [1/cm³s] → intrinsic carrier concentration
 τ_g → minority carrier lifetime ~ 1/N_{generation centers}

(2) Field-Assisted Generation: tunneling (trap-assisted and band to band)



Example:

- effective volume $V_{\text{eff}} = A_{\text{eff}} \cdot W_{\text{depletion}}$
 $V_{\text{eff}} \sim 1\text{mm}^2 \cdot 50\% \cdot 4\mu\text{m}$
- $\tau_g \sim 10\text{ms}$ (good quality technology)
- Prob. to trigger avalanche P_{01}
 $P_{01}^e \sim 100\%$ for electrons
 $P_{01}^h \sim 1/2 P_{01}^e \sim 50\%$ for holes

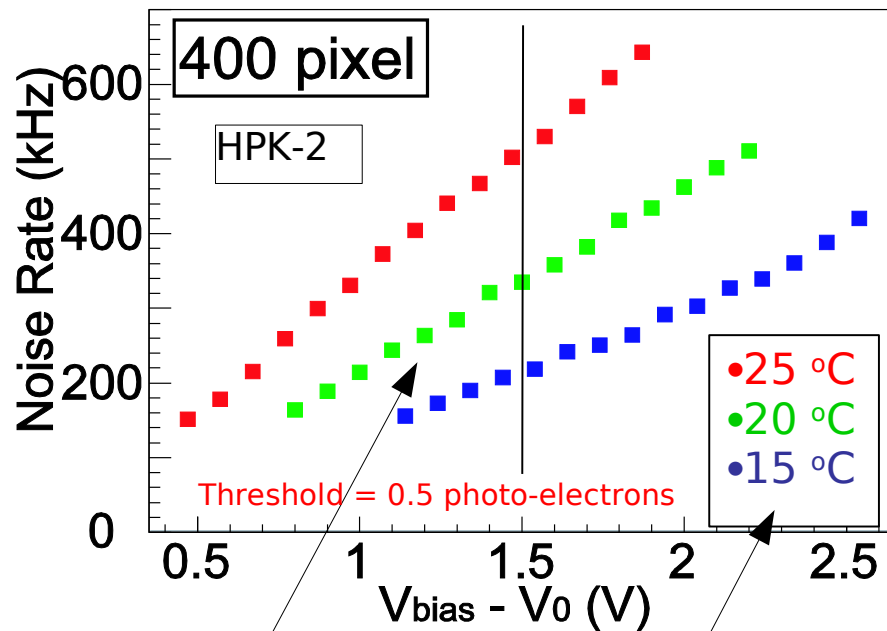
→ Dark rate $\sim V_{\text{eff}} P_{01} / \tau_g \sim 2\text{MHz}$ (n+/p: e trigger the avalanche in depl. region)
 $\sim 1\text{MHz}$ (p+/n: h trigger the avalanche in depl. region)

Dark count rate

Critical issues: • quality of epitaxial layer
• gettering techniques

Hamamatsu device (1mm²)

S.Uozumi – Vienna VCI 2007



NOTE:
T dependence

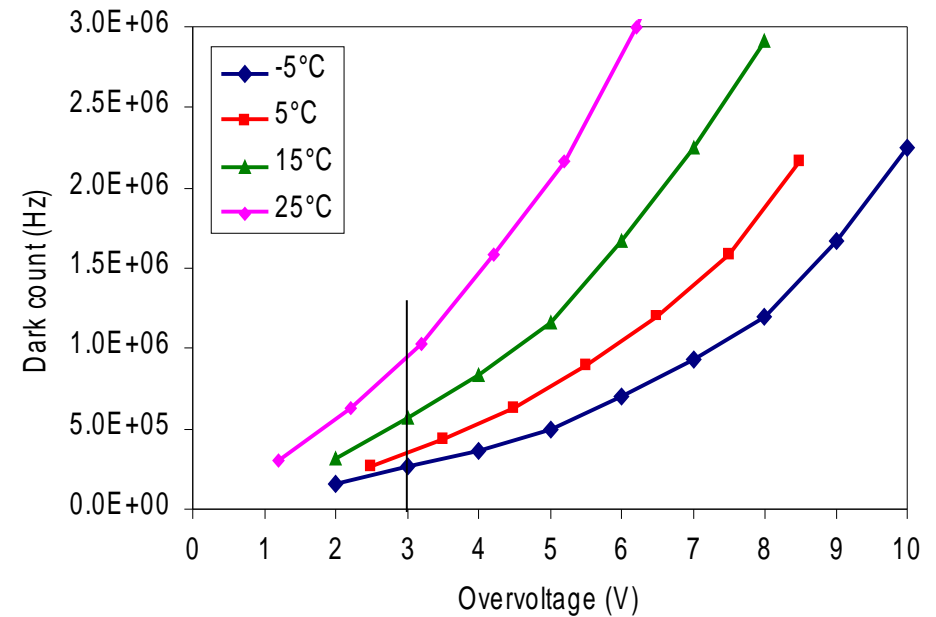
NOTE:

~ linear dependence due to $P_{01} \propto \Delta V$

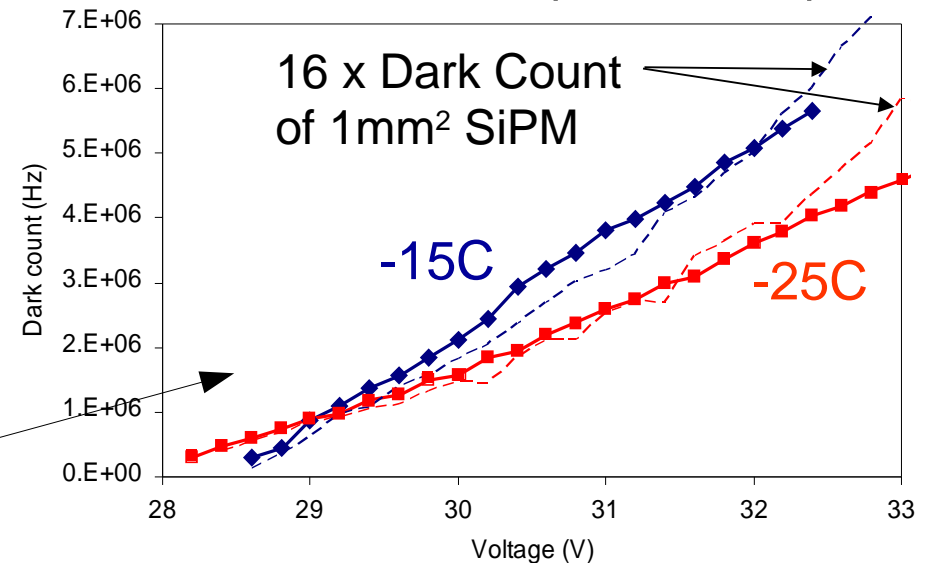
~ scales with active surface

~ non-linear at high ΔV due to additional rate from cross-talk ($\propto \Delta V^2$)

IRST device (1x1 mm²)

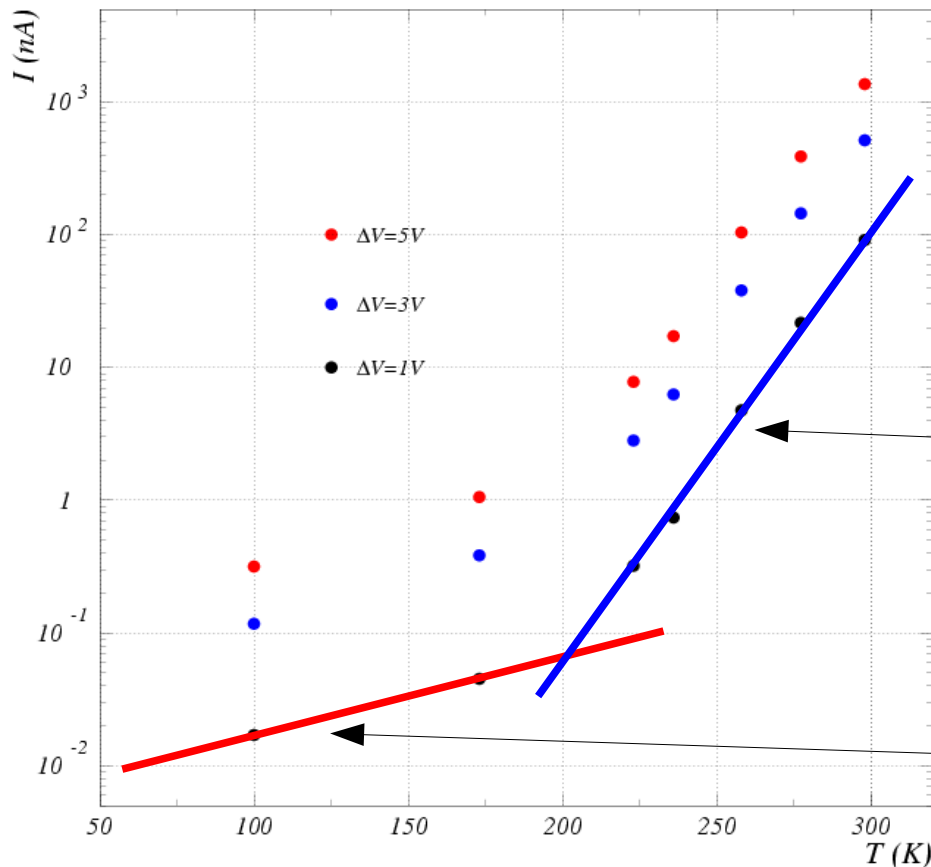


IRST device (4x4 mm²)



T dependence: Dark Current

Data (IRST devices)
(fixed over-voltage)



Dark rate sources:

1. Diffusion

I_{reverse} by minority carriers: negligible at room T

2. SHR (Field Enhanced)

Rule of thumb: factor $\times 2/8k$ (at fixed Over-voltage)
Dominates at room T

$$I_{\text{reverse}} \propto T^2 \exp\left(\frac{-E_g}{2K_B T}\right)$$

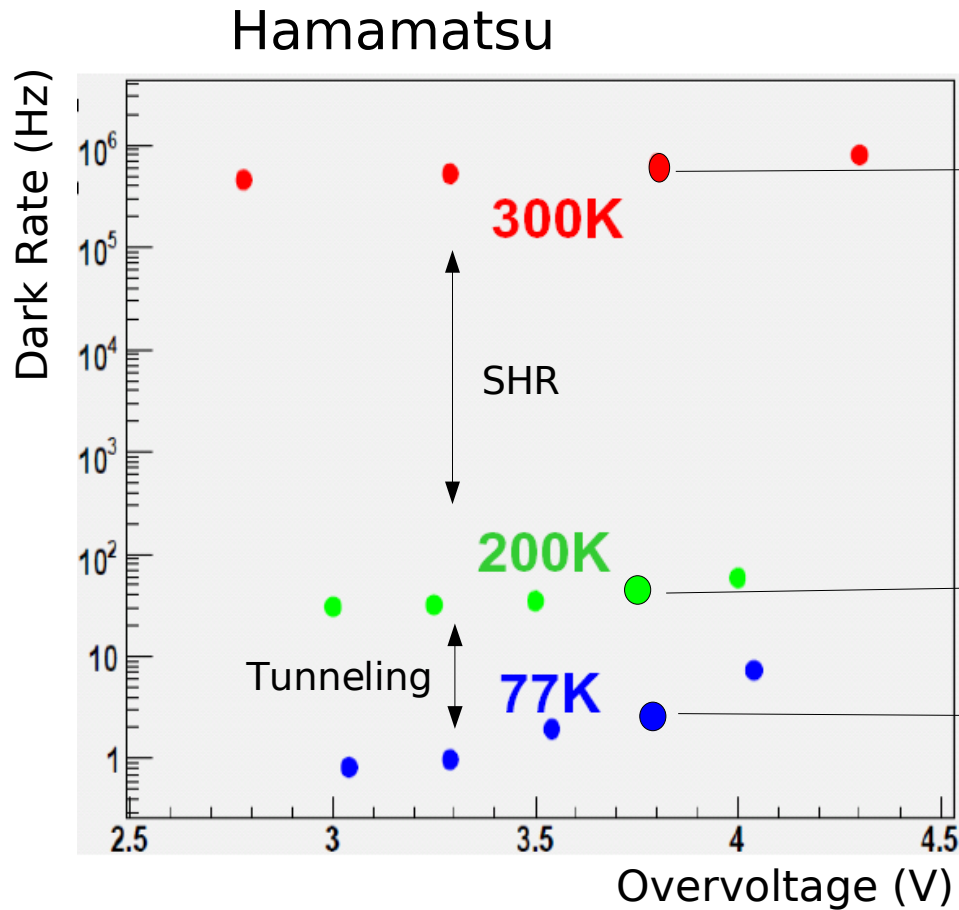
3. Band to band Tunnel

Strong dependence on the Electric field profile
May dominate at low T

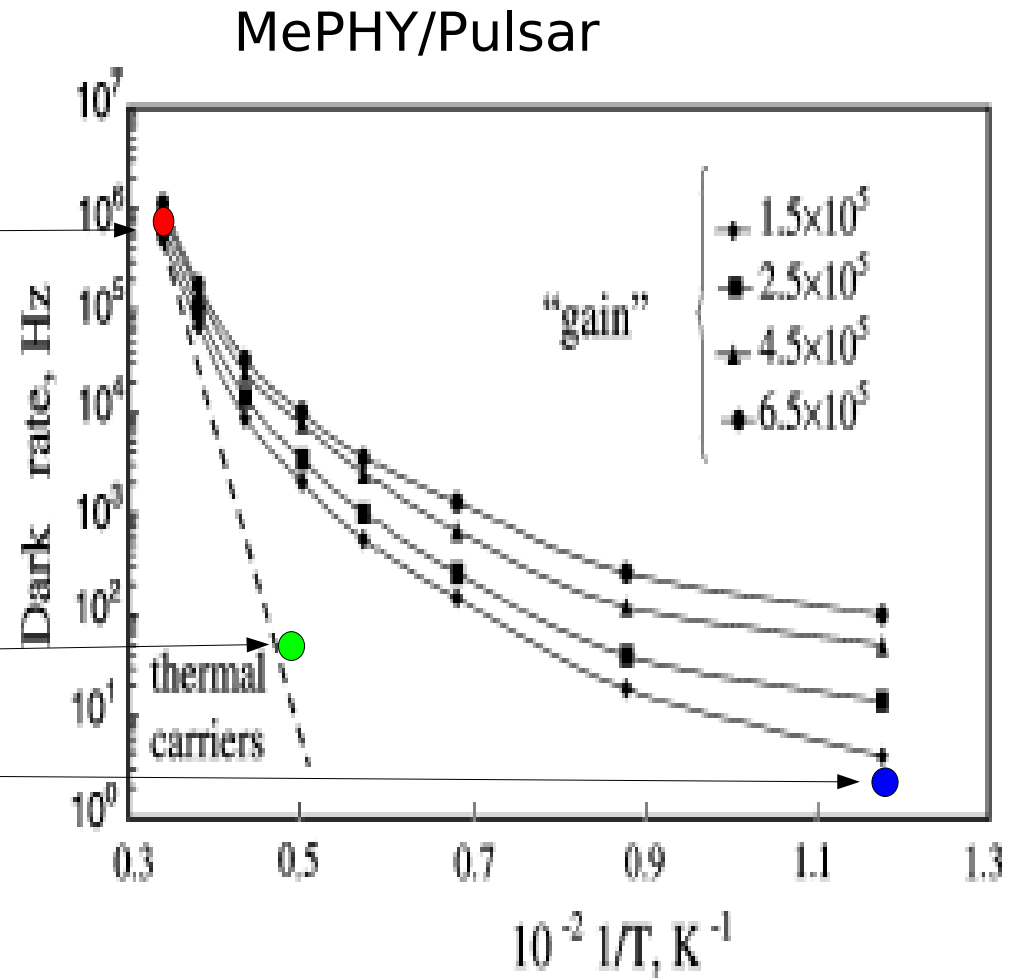
G.Collazuol

Acknowledgments: A.Baldini, A.Brez – INFN Pisa

T dependence: Dark rate



H.Otono – PD07



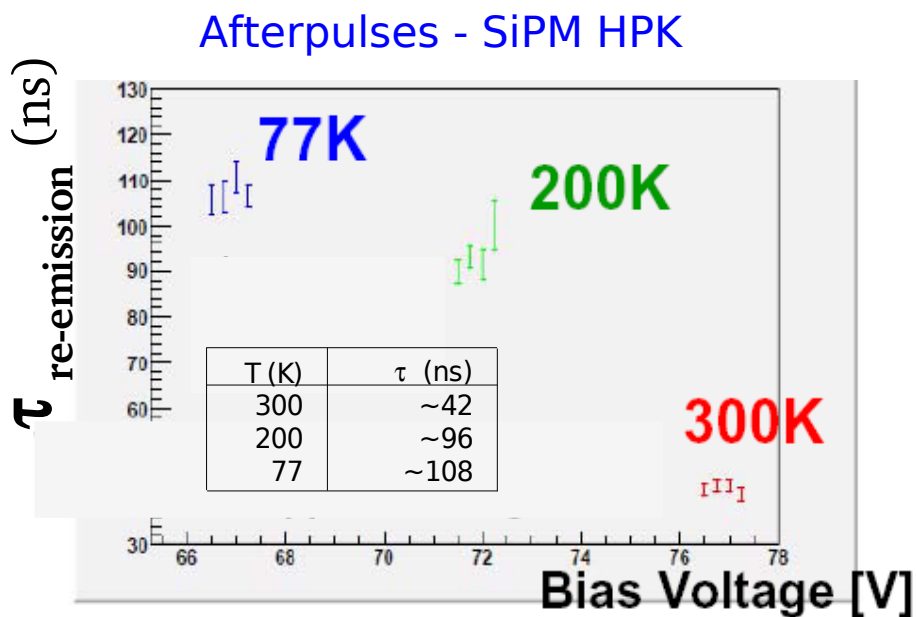
Dolgoshein et al, NIM A 442 (2000)

Electric field engineering and silicon quality
make huge differences in dark noise as a function of T

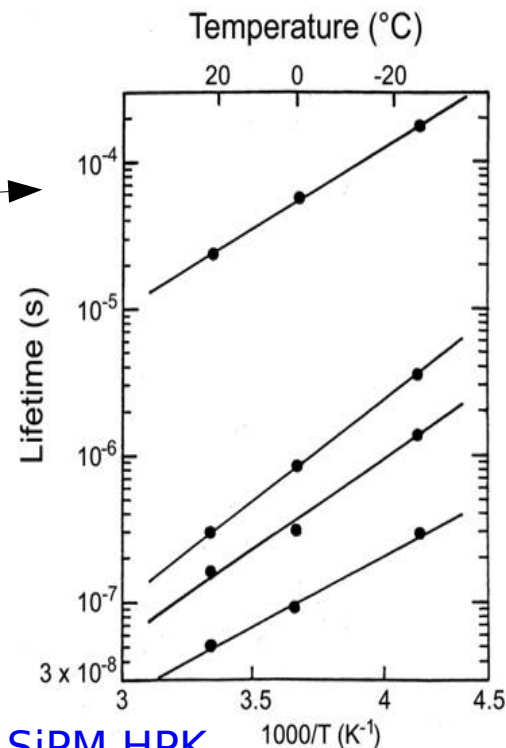
T dependence: after-pulsing, cross-talk

After-pulses: increases at low T

Trap lifetime decreases as T increases



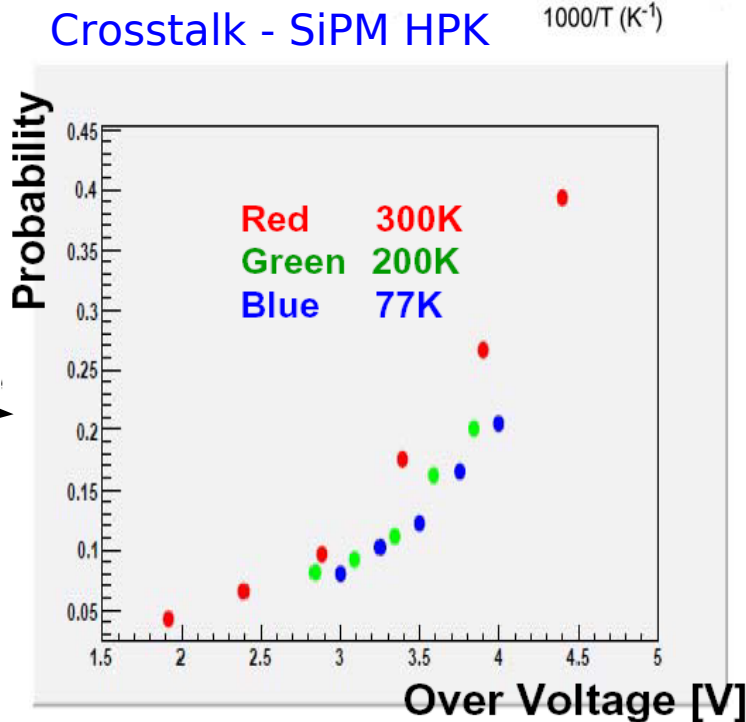
H.Otono - PD07 28 June 2007



S.Cova, A.Lacaita,
G.Ripamonti, IEEE EDL (1991)

Crosstalk: decreases at low T

Observed slight reduction at low T



(due to lower PDE for long wavelength photons which dominate the carrier luminescence spectrum)

Single photon timing resolution

Detailed studies about timing of Single Photon Avalanche Diodes (SPAD) by [S.Cova et al.](#)

Fast component (time scale few 10ps)
main resolution peak width

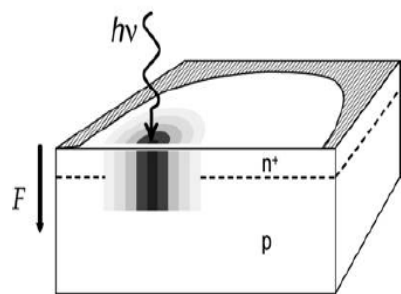
Statistical fluctuations in the Avalanche:

- **Vertical** build-up (**minor** contribution)
- **Horizontal** propagation (**major** contribution)
 - via Multiplication assisted diffusion (dominating contribution)
 - via Photon assisted propagation

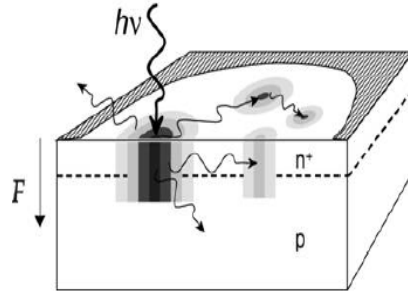
[A.Lacaita et al. APL and El.Lett. 1990](#)

[PP.Webb, R.J. McIntyre RCA Eng. 1982](#)

[A Lacaita et al API 1997](#)



Multiplication assisted diffusion

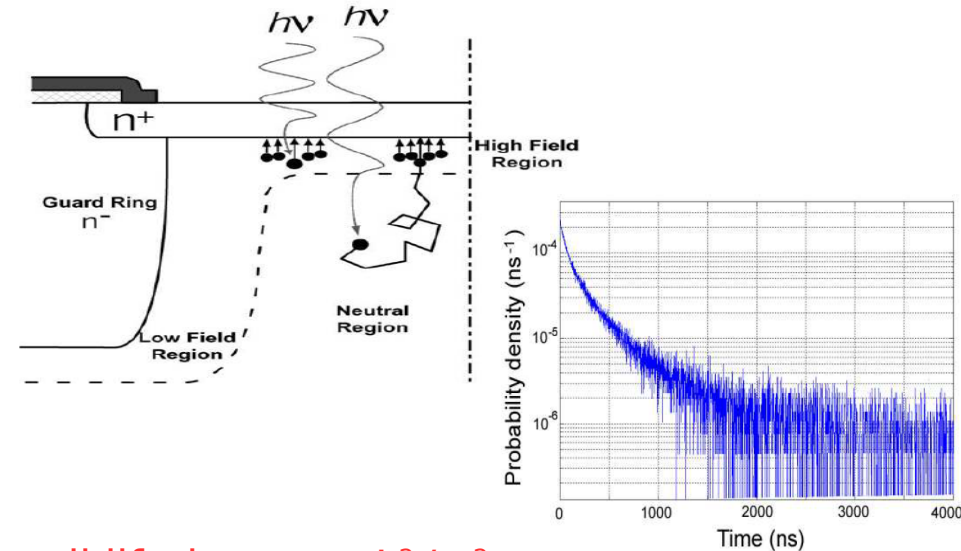


Photon assisted propagation

Slow component (time scale ns)
minor non gaussian tails

Carriers photogenerated in the neutral regions beneath the junction and reaching the electric field region by diffusion

[G.Ripamonti, S.Cova Sol.State Electronics \(1985\)](#)



tail lifetime: $\tau \sim L^2 / \pi^2 D$

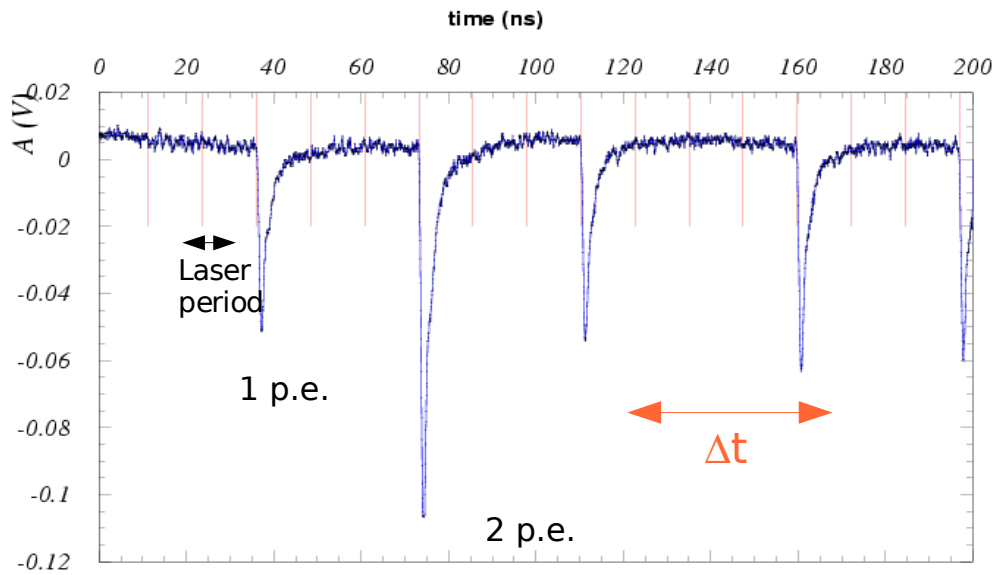
L = effective neutral layer thickness
D = diffusion coefficient

[S.Cova et al. NIST Workshop on SPD \(2003\)](#)

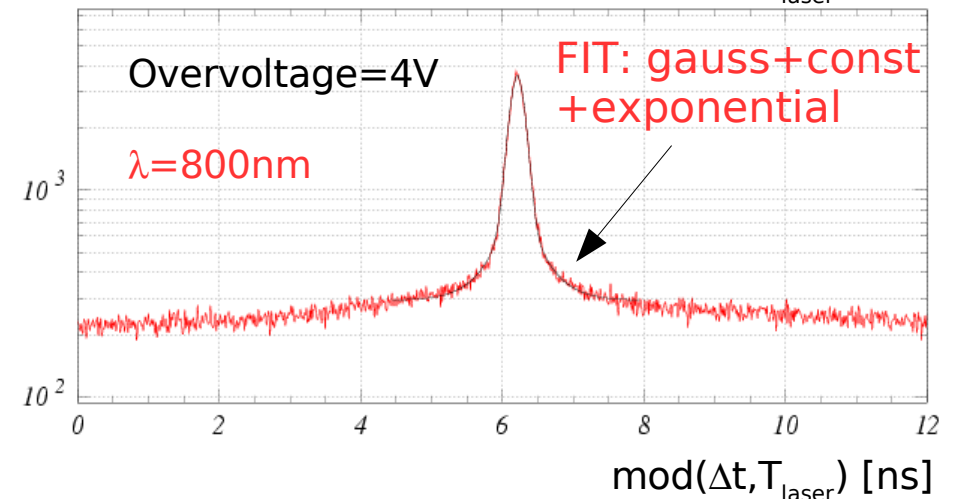
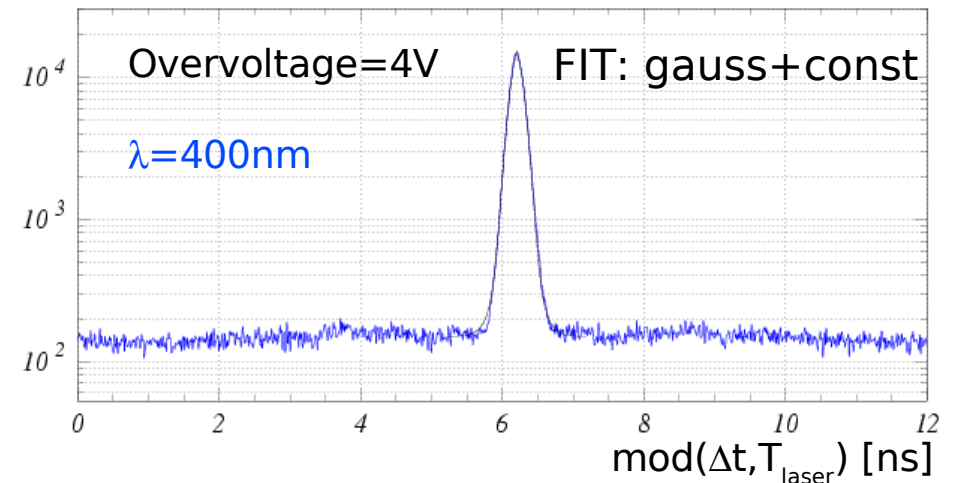
High overvoltage → high time resolution

Short wavelengths → high resolution (no tails)

Single photon timing resolution



Gaussian + Tails (long λ)
 rms \sim 50-100 ps
 $\sim \exp(-t / O(\text{ns}))$
 contrib. several %
 for long wavelengths

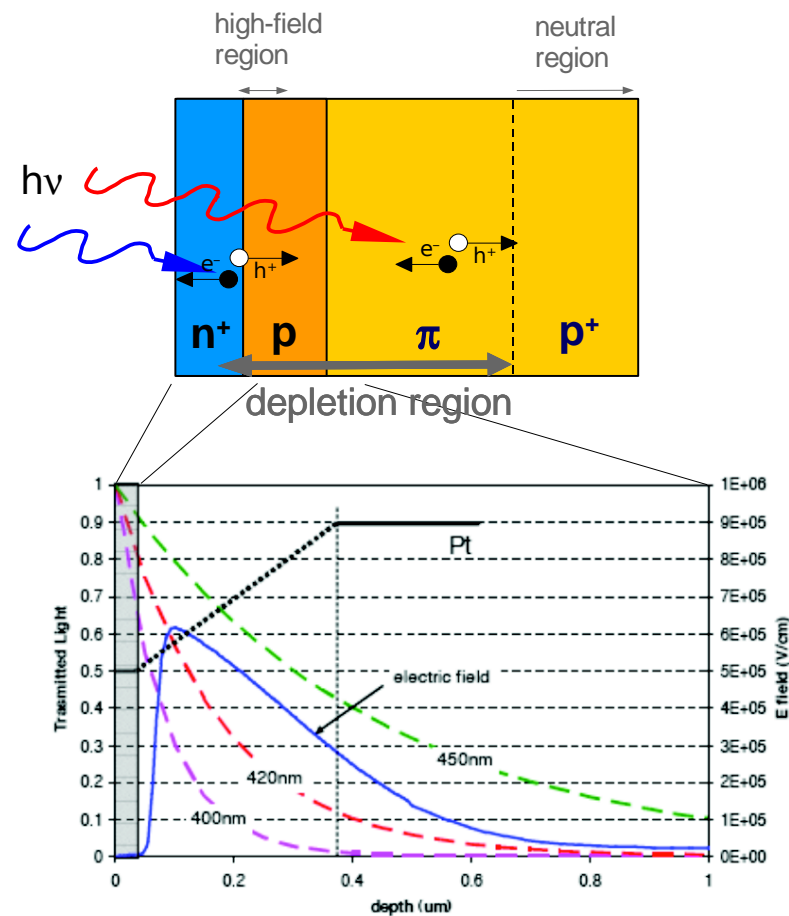
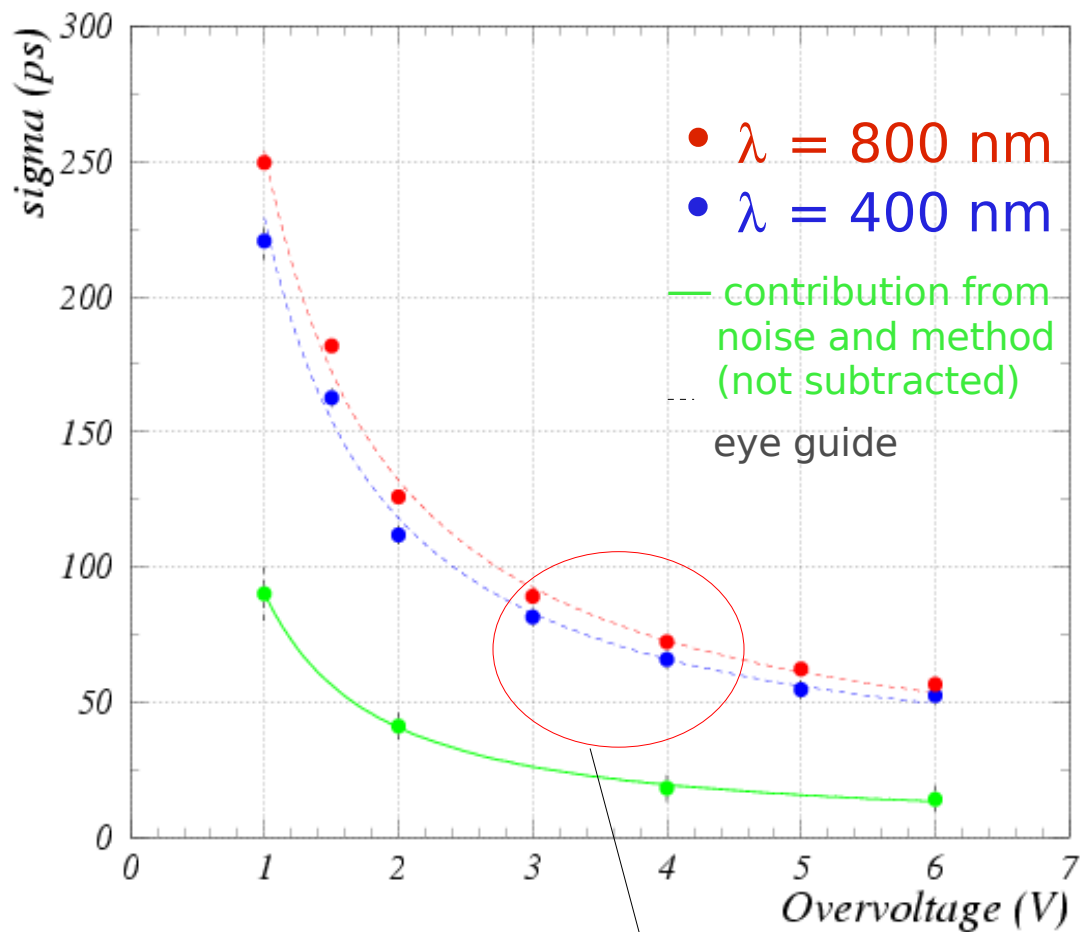


fit gives reasonable χ^2 with an additional exponential term $\exp(-\Delta t/\tau)$

- $\tau \sim 0.2 \div 0.8 \text{ ns}$ in rough agreement with diffusion tail lifetime: $\tau \sim L^2 / \pi^2 D$ if L is taken to be the diffusion length
- Contribution from the tails $\sim 10 \div 30\%$ of the resolution function area

Distributions of the difference in time between successive peaks (modulo the measured laser period $T_{\text{laser}} = 12.367 \text{ ns}$)

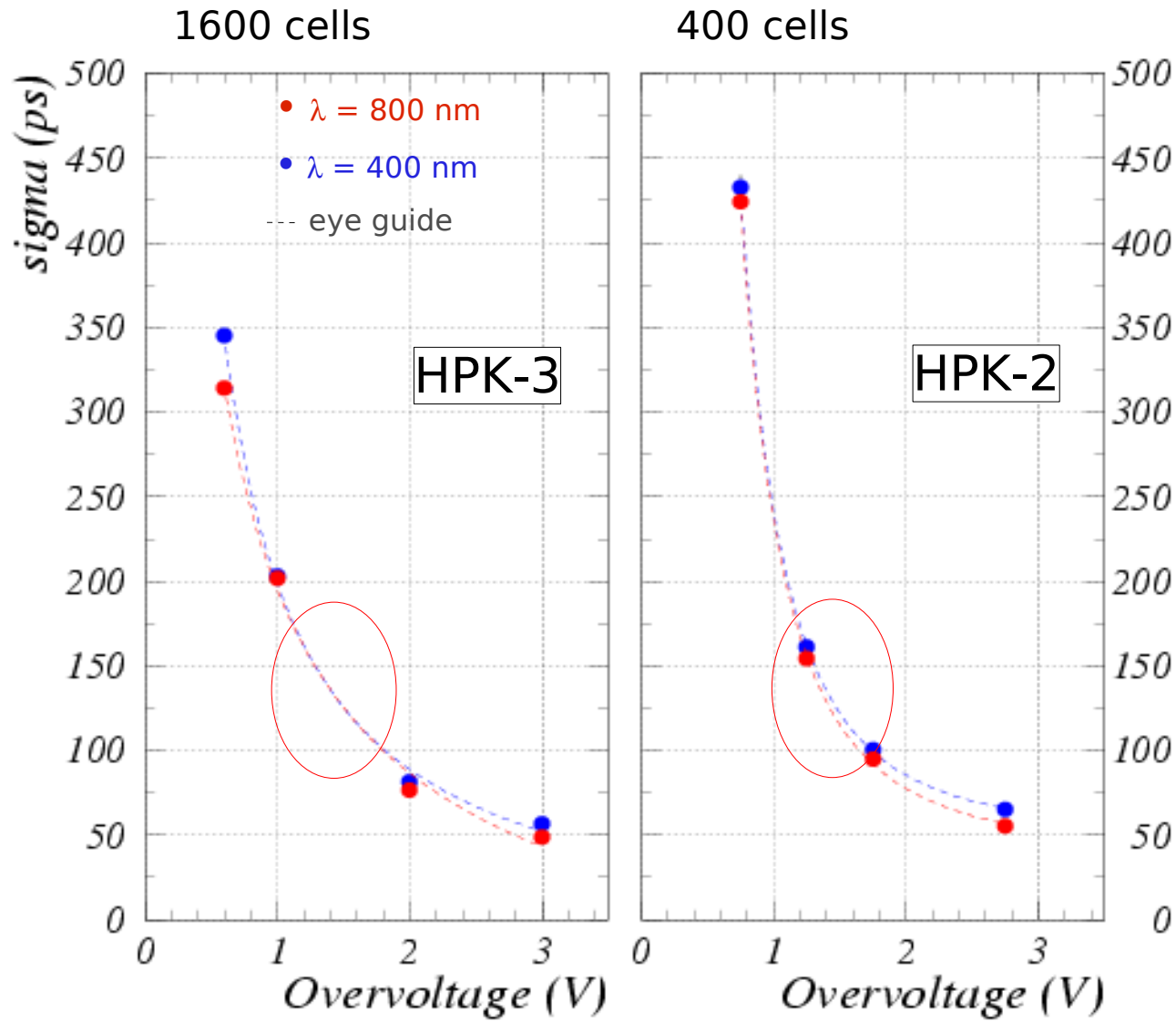
IRST – single photon timing



G.Collazuol et al.

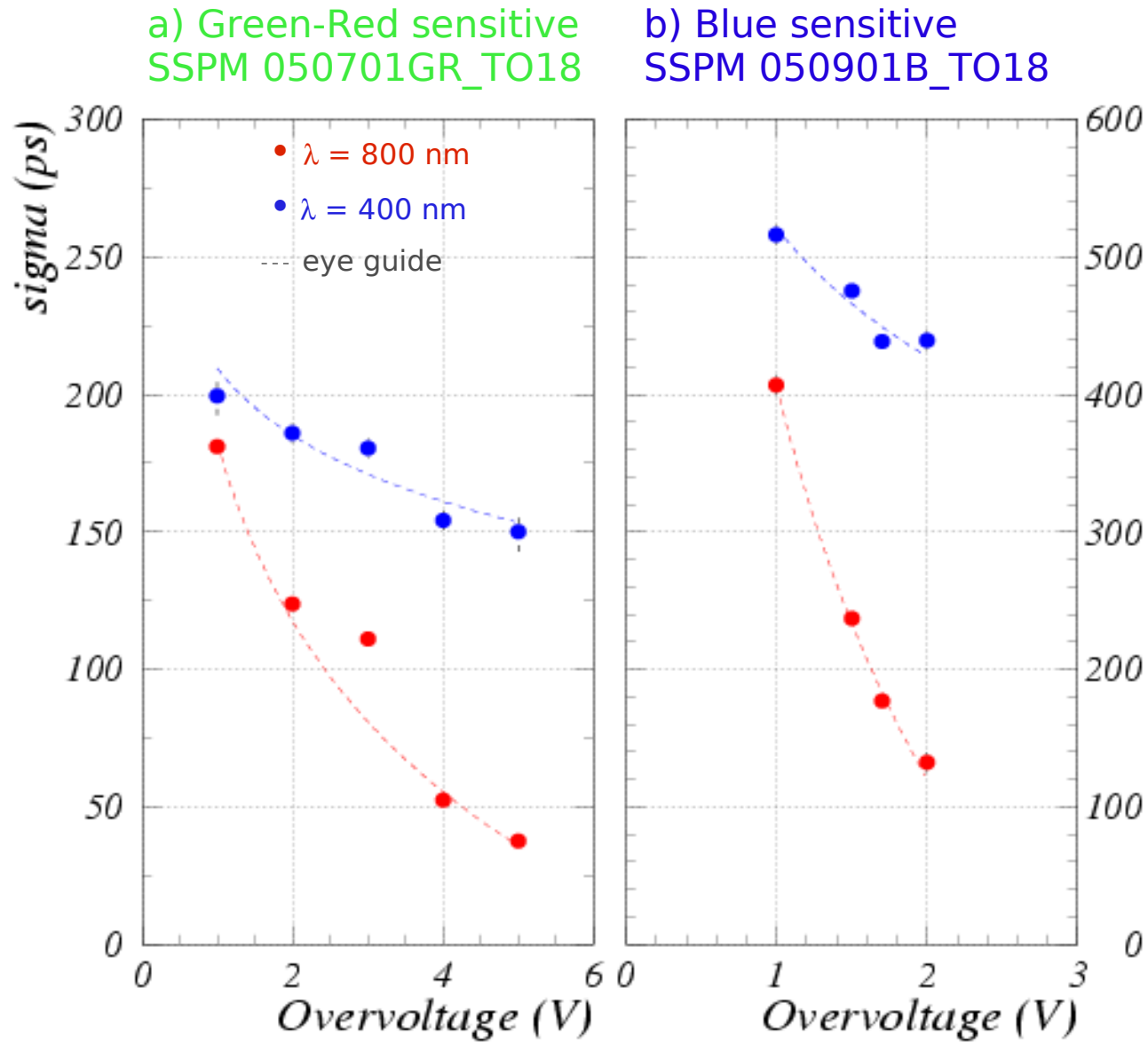
Typical working region

Hamamatsu – single photon timing



G.Collazuol (unpublished)

CPTA/Photonique – single photon timing



Two different structures:
a) thick n⁺/p
b) p⁺/n deep junction

Carrier trapping ?

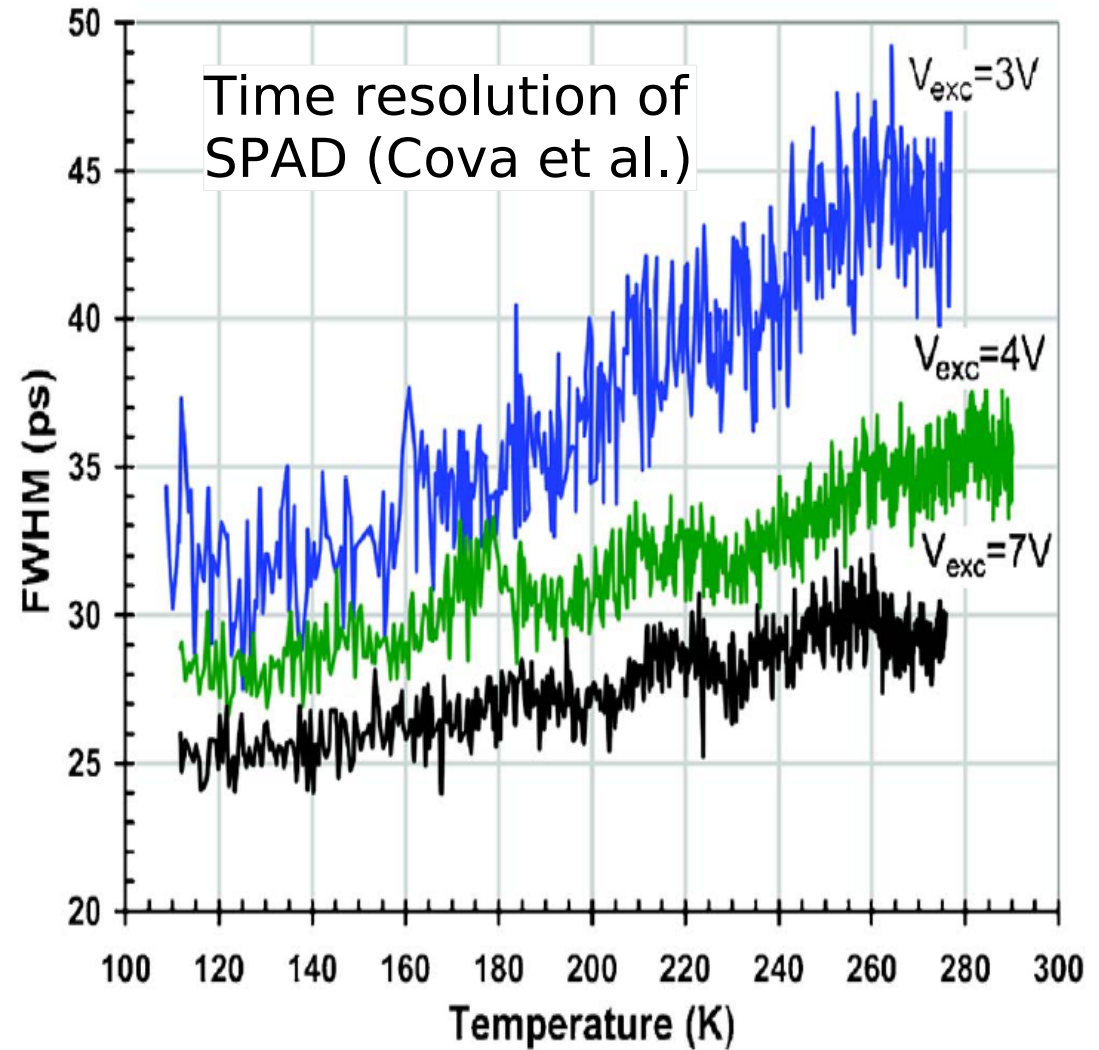
G.Collazuol (unpublished)

T dependence: PDE, timing (SPAD devices)

Timing: better at low T

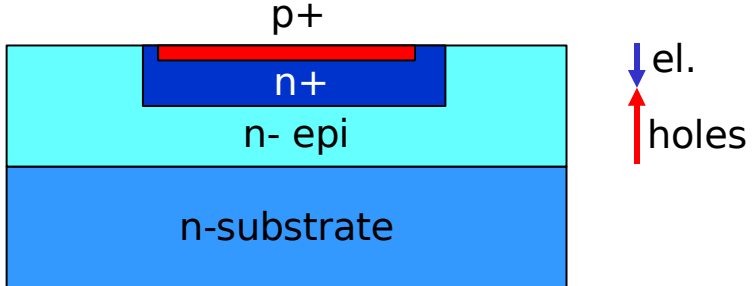
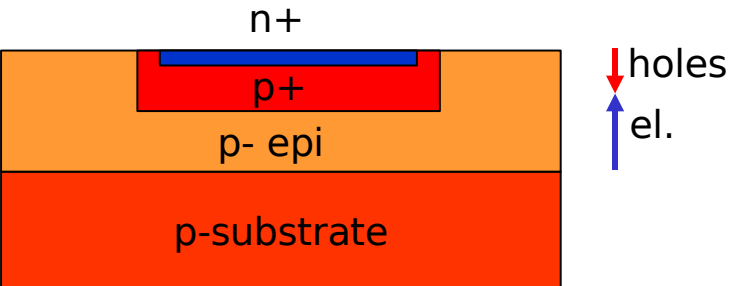
Lower jitter at low T due to higher mobility

(Over-voltage fixed)



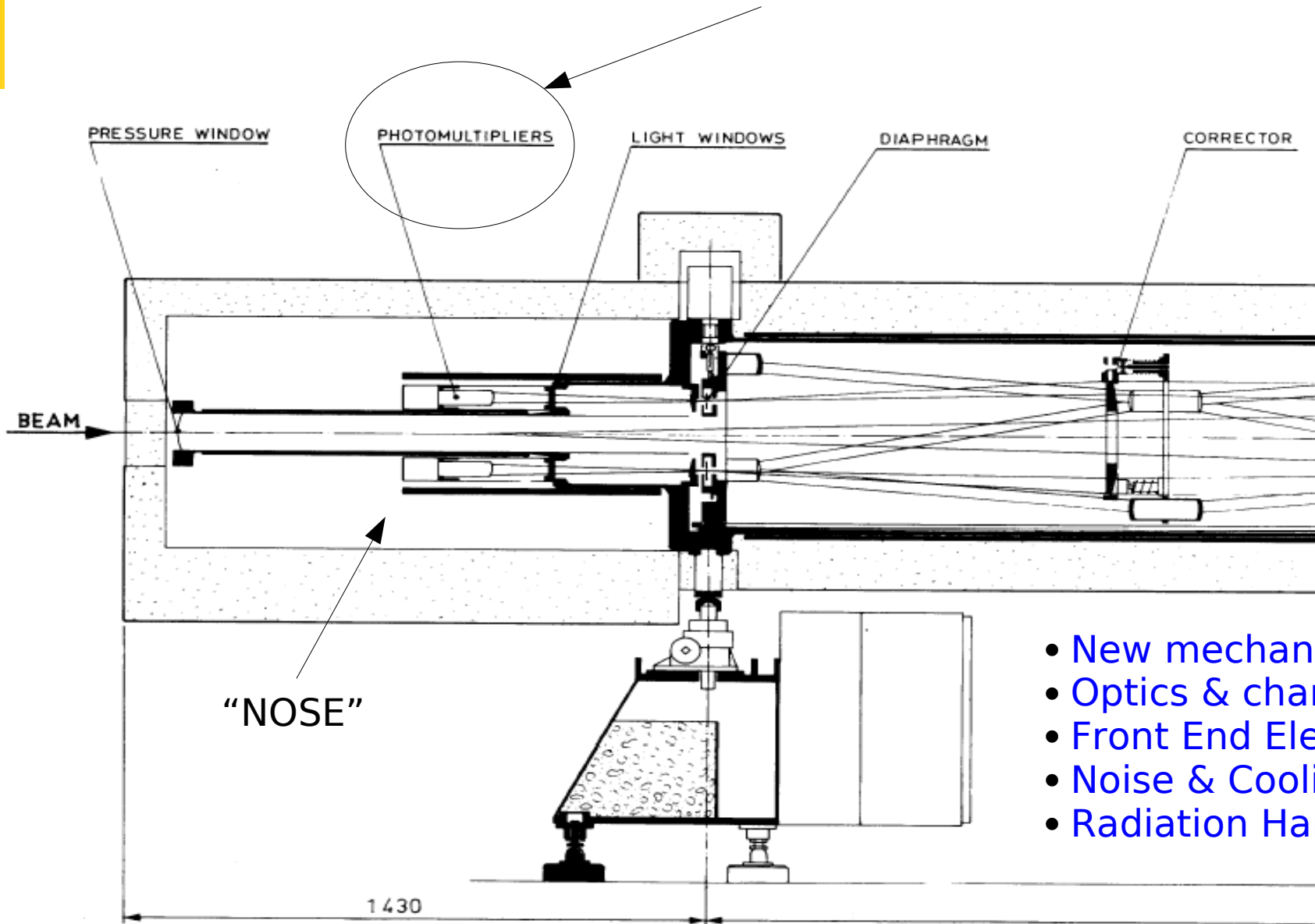
I.Rech et al, Rev.Sci.Instr. 78 (2007)

Comparison between SiPM

Product.	Hamamatsu	IRST
Type		
Gain	$10^5 - 10^6$	$10^5 - 10^6$
PDE	30-70% (UV)-blue-green	30-70% (blue)-green-IR
Noise	200kHz - 1MHz	~ HPK x 2
After-pulse	~ 10%	~ 1%
Cross-talk	~ 10%	~ 1%
Timing	~ 100 ps	~ 50 ps

NOTE: in the standard working V_{bias} range

Back to the CEDAR readout detector



- New mechanics
- Optics & channel density
- Front End Electronics
- Noise & Cooling
- Radiation Hardness

The new mechanics of the CEDAR "nose"

CEDAR "nose" new mechanics (additional T's) for allowing:

1. to tune of **optics** of the 8 Cerenkov **light spots** out of the quartz windows

→ light spot widening is **mandatory for the PMT readout**:

need at least x5 surface for reducing the average anode current of PMT

→ light spot smaller for readout with SiPM

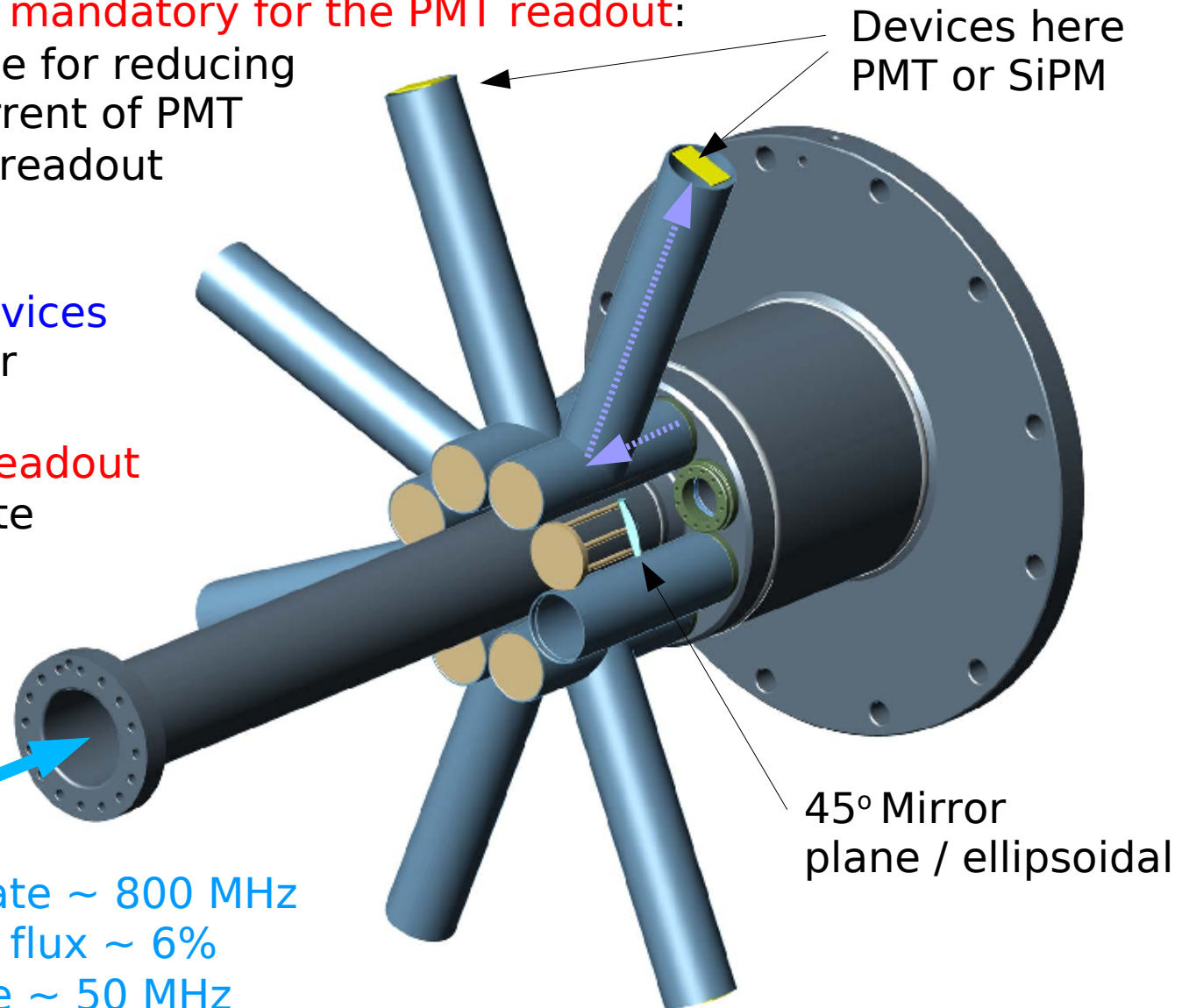
2. simple **cooling of the devices**

(T's are vacuum tight for thermal insulation)

→ **mandatory for SiPM readout** to reduce dark count rate

3. to keep devices in the **peripheral beam halo**

→ reduce radiation damage effects on SiPM

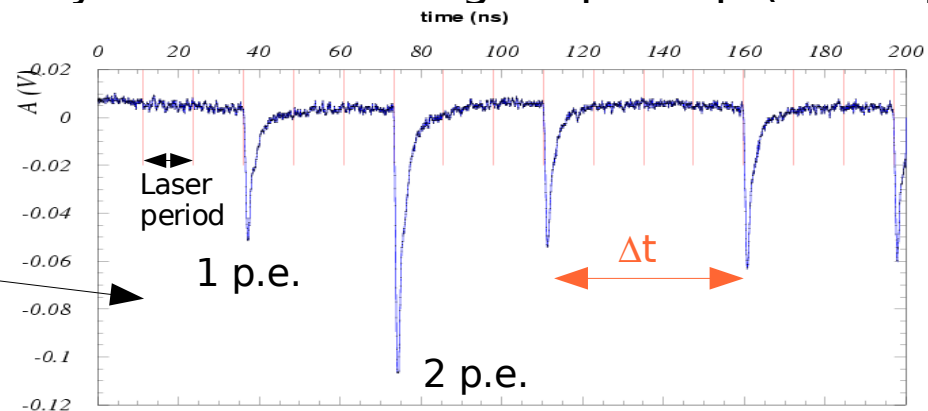


The Cerenkov light optics: PMT vs SiPM

SiPM can stand very high photon rates concentrated on small surfaces:

- recovery time is not an issue due to the hundreds of independent cells per mm^2
- the maximum rate per SiPM is limited by the effect of signal pile-up (\rightarrow shaping) on performances (eg timing)

Eg: SiPM's with cells $50 \times 50 \mu\text{m}^2$ in size still perform optimal counting and timing working at a single photo-electron rate of $20\text{MHz}/\text{mm}^2$



SiPM dark count rate scales with active surface

➔ New optics to concentrate the cerenkov light on the smallest area
Minimum spot surface $\sim 12 \times 12 \text{ mm}^2$ ($\frac{1}{2}$ x original)

PMT cannot stand high photon rates concentrated on small surfaces:

Eg: a single PMT (gain 2.5×10^6) covering 1 cerenkov light spot should stand on average $50\mu\text{A}$ which is of the order of the typical max. average current rating

But dark rate is not an issue for PMTs'

➔ New optics to produce larger light spot
Reasonable spot surface $\sim 40 \times 40 \text{ mm}^2$ (5 x original)

Comparison SiPM vs PMT

for applications of photon counting and timing at high rates

	PMT	SiPM
Reference device (eff. area)	HPK R7600 (18x18 mm ²)	HPK S10362-11-50C (1x1 mm ²)
Gain (G)	$\geq 10^6$	$\geq 10^6$
$\delta V/V$ for $\delta G/G=1\%$	3×10^{-4}	6×10^{-4}
δT for $\delta G/G=1\%$	5° C	0.3° C
Max average anode current	100 μ A (350 mm ²)	3 μ A (1 mm ²)
Efficiency (on active area)	~25% @ 400nm ~40% (UBA)	~95% @ 400nm
Collection efficiency	70%	40% to 80%
Time resolution	~300ps	50ps to 100ps
Dark noise (1 p.e.)	few kHz	0.5 MHz @room T
After-pulse (thr. @ 1 p.e.)	1 % level	10 % level
B-field immunity	No	Yes
Radiation damg.	No (also at single photon level ?)	Yes

Gain = $C_{\text{cell}} \times \Delta V$

20MHz limit to avoid signal pileup. Not mandatory: can use proper shaping !!!
SiPM can stand at least x10 more rate per unit area than PMT

Approx. $\propto \Delta V$

Fill factor (cell geometry)

Approx. $\propto \Delta V^{-1}$

Approx. $\propto \Delta V$

Approx. $\propto \Delta V^2$

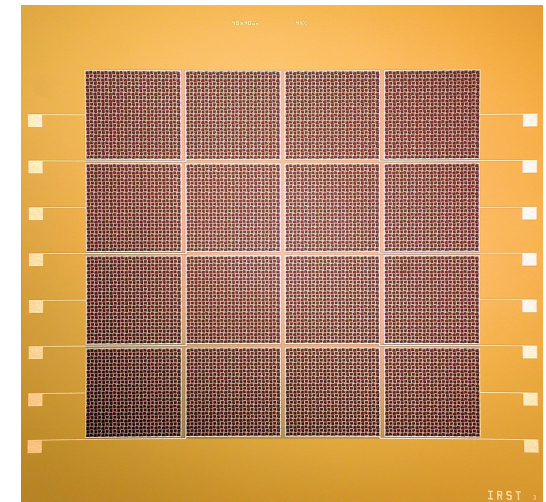
ΔV is the over-voltage
 $= V_{\text{bias}} - V_{\text{breakdown}}$

SiPM readout: granularity and rates

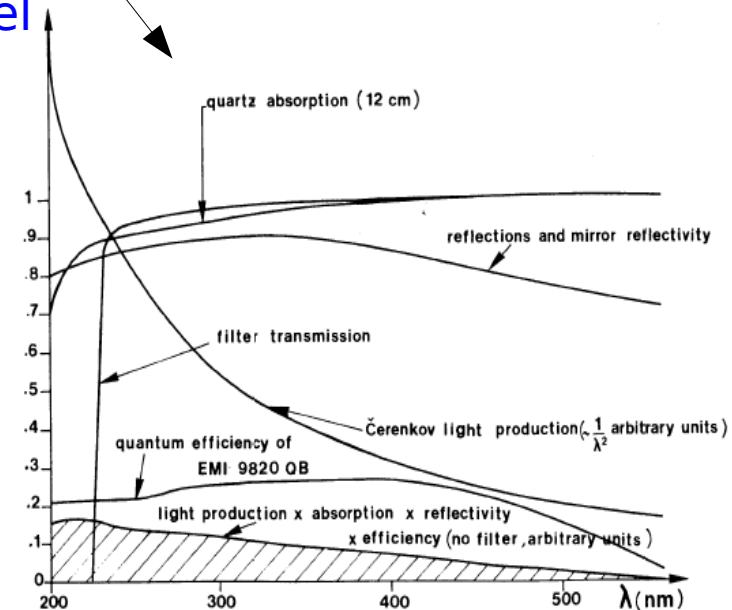
- Assume to collect light on a spot area of $12 \times 12 \text{ mm}^2$ covered by a matrix of 4×4 square SiPM's each of dimension $3 \times 3 \text{ mm}^2$ and 900 cells ($100 \times 100 \mu\text{m}^2$)
 - PDE $\sim 50\%$ ($> \times 2$ efficiency of PMT, but less sensitivity to UV; PDE and Č light spectrum shape)
 - 16 SiPMs (channels) per spot
- 10 Cerenkov photons per Kaon @ 50 Mhz result (accounting for PDE shape) in an average of 3p.e. @ 50 MHz (K rate) per spot (24 p.e. in total)
 - 10MHz of ≥ 1 p.e. (ie over 0.5 p.e. thr.) per channel
- Kaon detection efficiency with 3p.e. per spot and the old logic of 6/8 or 7/8 spot coincidences is well above 95%
- Single Kaon crossing time would be measured with a resolution better than $\sim 15 \text{ ps}$ ($70 \text{ ps}/\sqrt{24}$)

NOTE:

with $\times 16$ granularity (i.e. 16×16 matrix of $1 \times 1 \text{ mm}^2$ SiPM) could possibly tag pions at 800MHz



Dead regions between SiPM on a SiPM matrix can be very small (few $10 \mu\text{m}$)



Fast FE Electronics for counting and timing

Ideal FE for a **high rate system**:

- 1) **current amplifier** or I-V converter: smallest Z_{in} (to exploit the fast component)
need low Gain $\sim x20$ (especially if SiPM working at low gain) \rightarrow high bandwidth
 \rightarrow inherently fast (time resolution of the device not to be spoiled)
- 2) **RC shaper**
 \rightarrow minimize signal occupancy (pile-up) per channel
 \rightarrow maximize the double pulse resolution (DPR $< 5ns$) } to minimize the Kaon tagging inefficiency
- 3) **sampling with FADC**
 \rightarrow sampling (8 bits) at 1GHz: time resolution better than 20 ps rms
and DPR better than 5ps are easy to obtain
 \rightarrow cost/channel $< 180 \$$

Minimum **number of channels** to be evaluated on the basis of:

- Max level of **inefficiency in kaon tagging due to pile-up**:
eg: DPR $\sim 5ns$ with $>1p.e.@10$ Mhz (signal) + $>1p.e.@1$ Mhz (noise) on 16 ch.
 \rightarrow inefficiency due to pile-up $\sim 5\%$
- Limit on **time resolution**: worsens with rate

NOTE:

1. up to now our tests with **voltage amplifier + sampling** were successful even at very high rates (20MHz, see "single photon timing resolution meas.", VCI 07)
2. at the moment we are testing the Time Over Threshold discrimination technique by exploiting the NINO chip (ALICE TOF, NA62 RICH) as an alternative FE chain: **SiPM + Preamplif. + ToT Discrim. + TDC**

SiPM Noise: dark count rate

Best technologies HPK and FBK-IRST: dark counts (DC) $\sim 0.5 - 1 \text{ MHz/mm}^2 @ T=25^\circ\text{C}$
→ 75 - 150MHz cts/spot @ threshold of 0.5 p.e. (at gain $G=10^6$) to be reduced by:

1. **cooling (moderate, but mandatory):**

at $T \sim 200\text{K} \rightarrow \text{DC} \sim 10 - 50\text{kHz cts / spot}$
(more than 3 orders of magnitude)

- Not worth going below 200K due to tunnel effect dominating.

- Easiest and cleanest solution: controlled N_2 flow in serpentine capillary tube to cool SiPM. Thermal insulation by vacuum
- Peltier is not so clean a solution.

2. **working at lower gain** to reduce DC

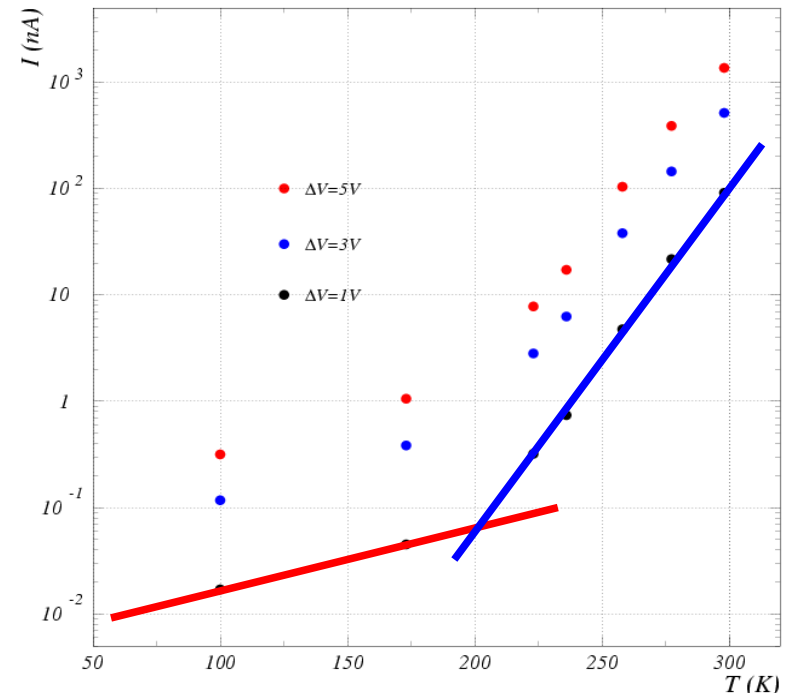
3. using **coincidences**: have on average ~ 24 p.e. per Kaon (8 spots)

• **After-pulses:**

not an issue (unless cooling below 120K):
 $\sim 2\% @ G=10^6 \rightarrow 1\text{MHz}$ additional per spot

• **Cross-talk:**

not an issue: well below 1% (FBK-IRST)



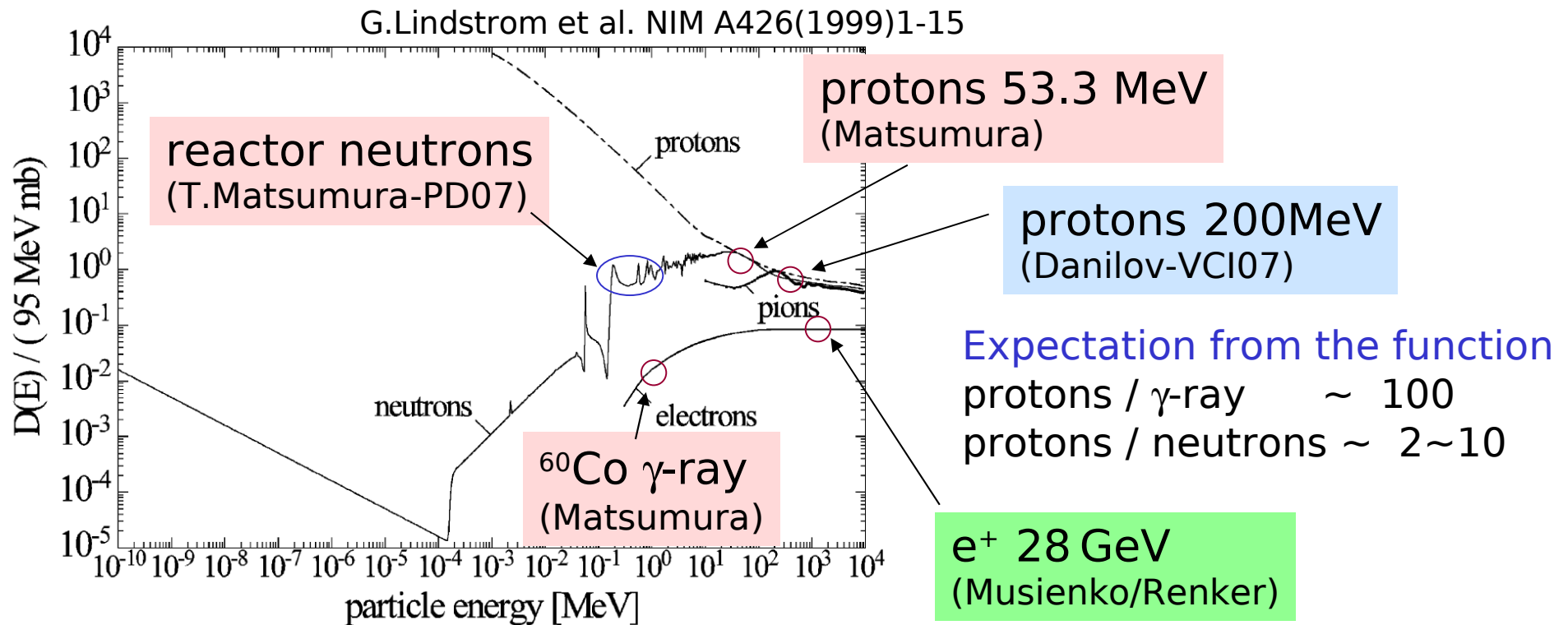
NOTE:

- FBK-IRST (n+/p) has $\sim \times 2$ noise than HPK (p+/n)
- T affects also $V_{\text{break-down}}$ ($\Delta V_{\text{BD}}/\Delta T \sim 80\text{mV/K}$) but Gain is the same at fixed overvoltage ΔV . PDE and Timing resolution improve at low T, worsen at low ΔV
- After-pulsing and cross-talk $\sim \Delta V^2$
Gain, PDE and dark rate scale $\sim \Delta V \rightarrow$ keep low ΔV
Timing resolution $\sim 1/\Delta V^\alpha$
- Cooling $\rightarrow T$ drifts \rightarrow stable working conditions

Radiation damage: two types

- Bulk damage due to Non Ionizing Energy Loss (NIEL) ← neutrons, protons
- Surface damage due to Ionizing Energy Loss (IEL) ← γ rays
(accumulation of charge in the oxide (SiO₂) and the Si/SiO₂ interface)

Assumption: damage scales linearly with the amount of Non Ionizing Energy Loss (NIEL hypothesis)



Examples of radiation tolerances for HEP and space physics

ATLAS inner detector ... 3×10^{14} hadrons/cm²/10 year
 $\sim 10^4$ hadrons/mm²/s

General satellites ... ~ 10 Gy/year

Radiation damage: effects on SiPM

1) Increase of dark count rate due to introduction of generation centers

Increase (ΔR_{DC}) of the dark rate:

$$\Delta R_{DC} \sim P_{01} \alpha \Phi_{eq} Vol_{eff} / q_e$$

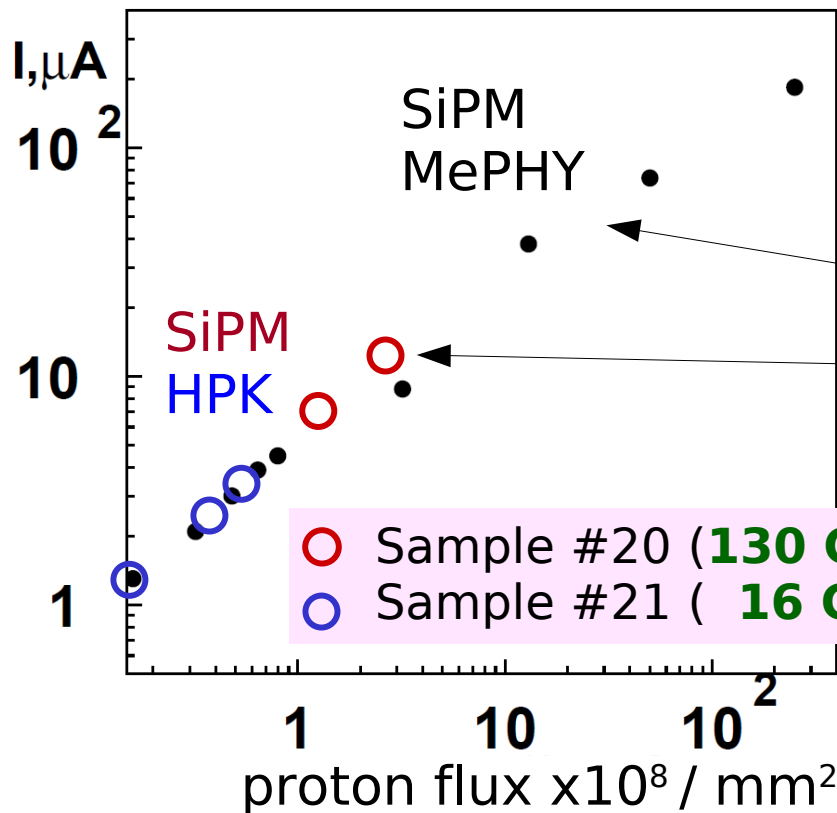
where $\alpha \sim 3 \times 10^{-17} \text{ A/cm}$ is a typical value of the radiation damage parameter for low E hadrons and $Vol_{eff} \sim Area_{SiPM} \times \epsilon_{geom} \times W_{epi}$

NOTE:

- The effect is the same as in normal junctions:
- independent of the substrate type
 - dependent on particle type and energy (NIEL)
 - proportional to fluence

2) Increase of after-pulse rate due to introduction of trapping centers

→ loss of single cell resolution → no photon counting capability



Indications from measurements:

- 1) no dependence on the device
similar effects found for SiPM from MePHY (Danilov) and HPK (Matsumura) (normaliz. to active volume)
- 2) no dependence on dose-rate
HPK (Matsumura)
- 3) n similar damage than p
- 4) p $\times 10^1$ - 10^2 more damage than γ



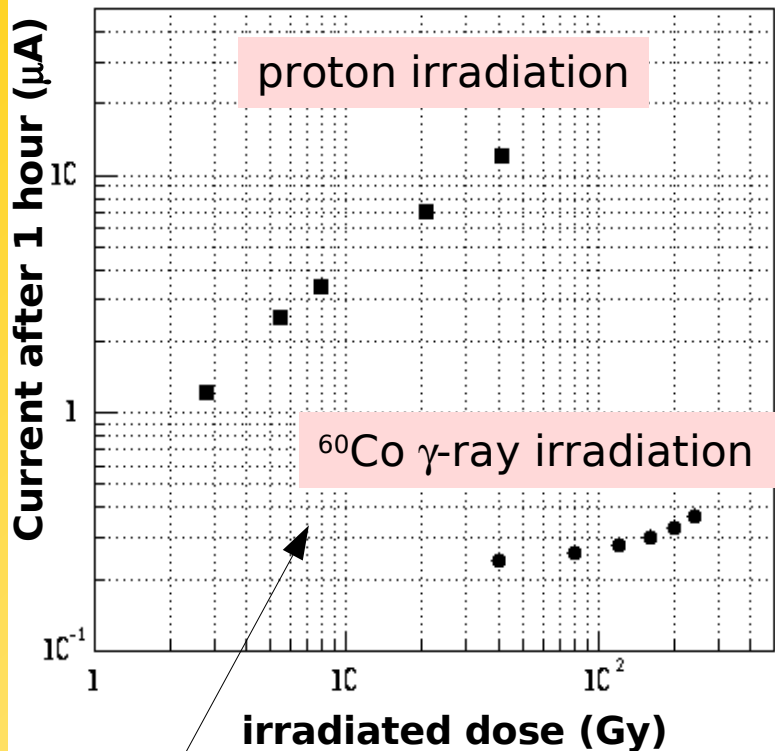
Damage comparison

2.3×10^5 p/mm²/s (130 Gy/h)

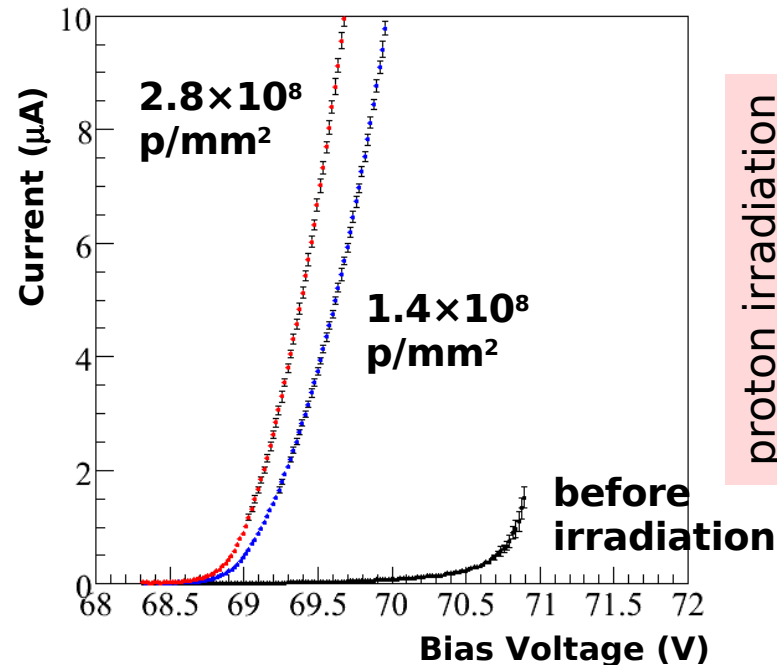
$I_{leak} @ (V_{op}, 1.4 \times 10^8 \text{ p/mm}^2) = 6.7 \mu\text{A}$

Damage effect ...
almost the **same** for
protons and neutrons

HPK devices
T.Matsumura – PD07

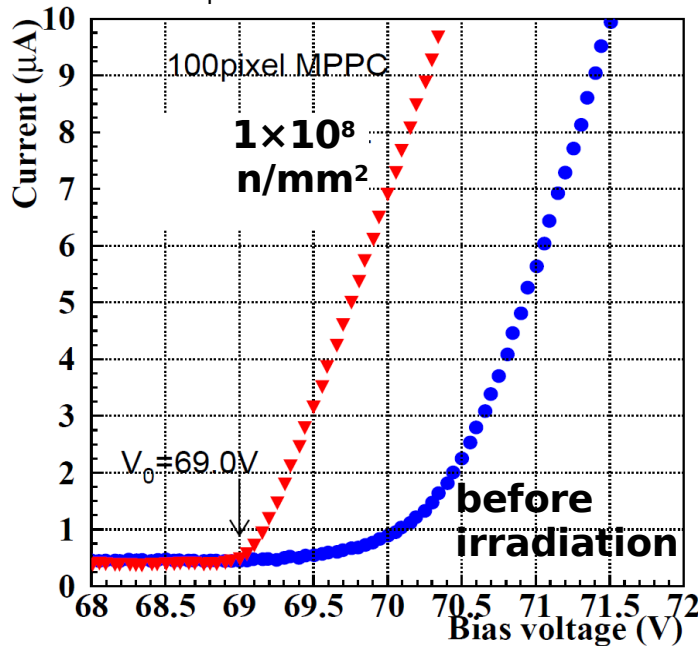


Damage effect ...
1~2 orders larger with protons
than γ-ray irradiation



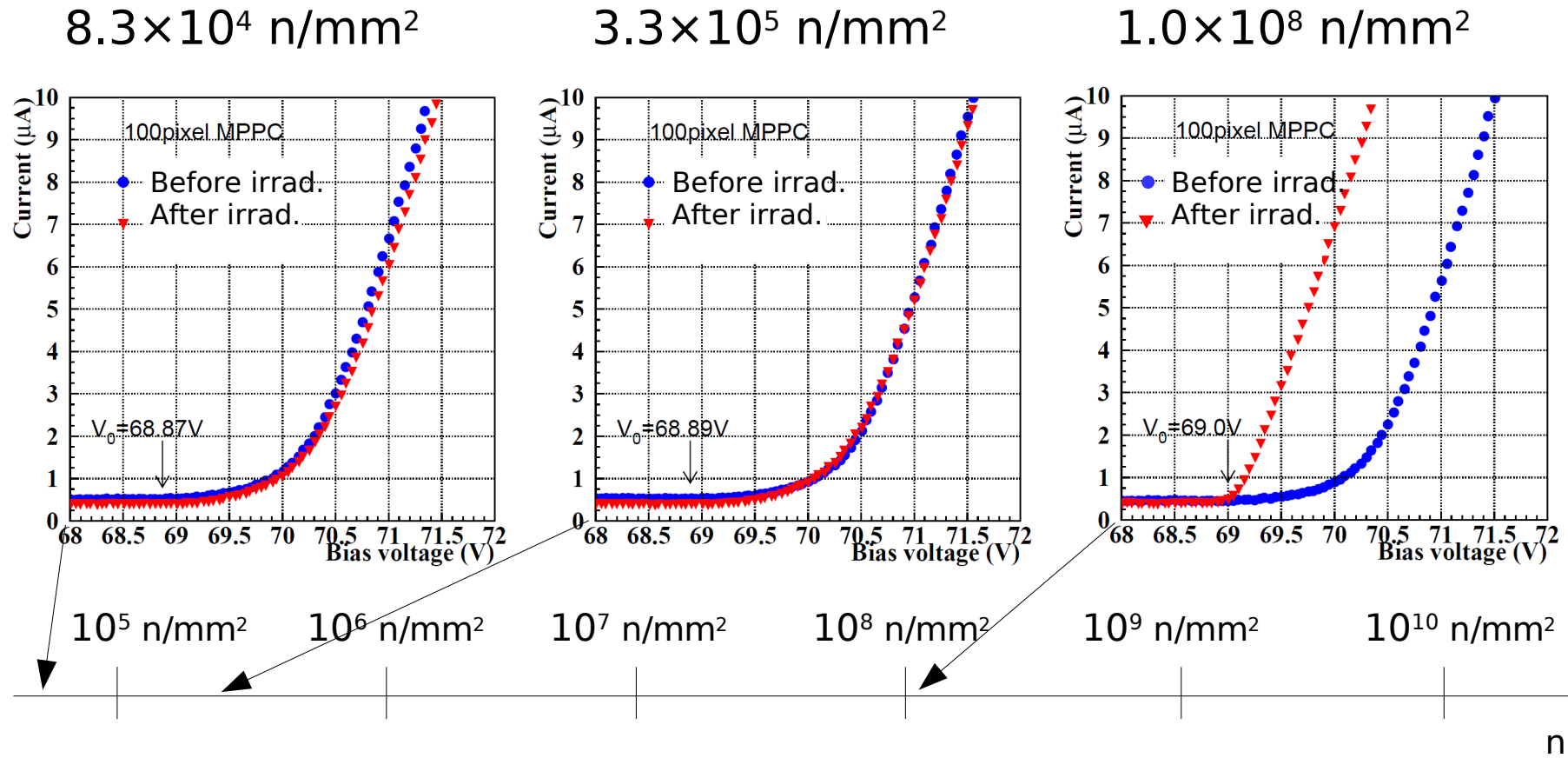
4.2×10^5 n/mm²/s

$I_{leak} @ (V_{op}, 1.0 \times 10^8 \text{ n/mm}^2) = 8.5 \mu\text{A}$



T.Matsumura – PD07

Radiation damage: neutrons (0.1 -1 MeV)



T. Matsumura – PD07

No significant change

Very rough estimate of the neutron flux in the beam halo (80cm from beam core) for 1 year run of NA62.

- NOTE: 1) huge uncertainties (n spectrum, HE)
 2) hadron shields still to be considered
 3) annealing and cooling effects on damages ?

I-V drastically change. Signal pulse is still there, but continuous pulse height. (No photon-counting capability)

No signal

More measurements and studies

G. Collazuol

Conclusions

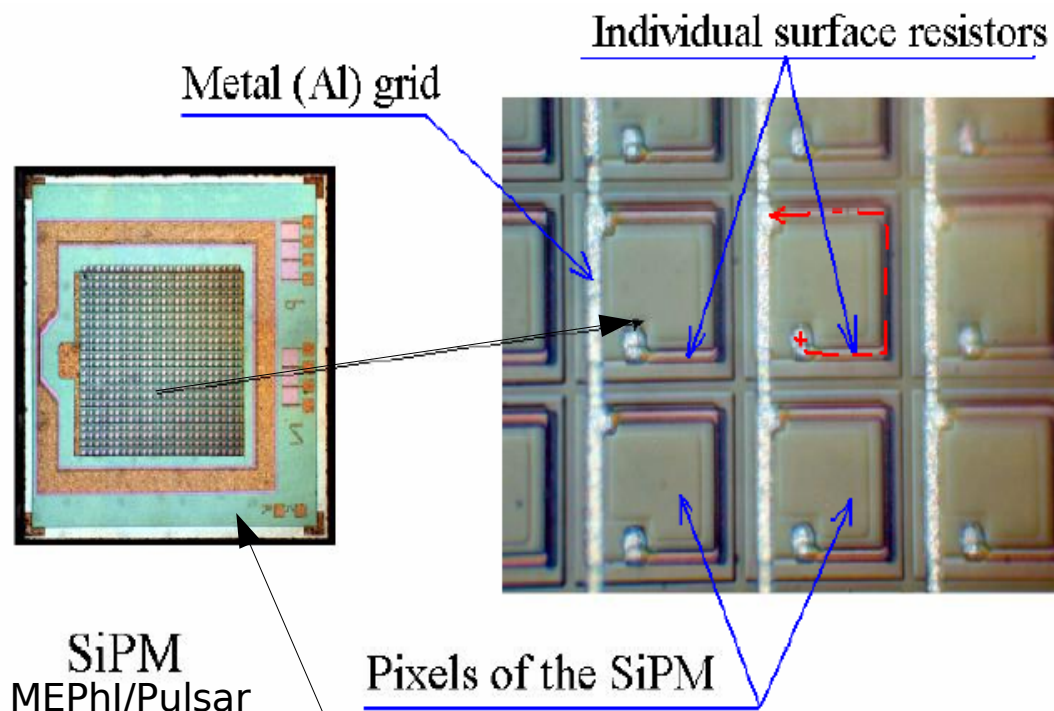
- We are studying the possibility of exploiting **Silicon Photo-multipliers as read-out detector** for a **Cerenkov differential counter** (CEDAR) that will tag Kaons in the high intensity, high energy hadron beam of the future experiment NA62 at CERN
- **Working principles and performances** of a few selected SiPM were summarized
- The main advantages in the use of SiPM are:
 - 1) their **good efficiency** and **very good time resolution** (at least x4 wrt PMT) which could be exploited in NA62 if a 2nd Cerenkov downstream detector will measure for each particle in the beam the crossing time with a resolution comparable with that of the CEDAR that is < 20ps rms
 - 2) their **lower cost** (at least x1/4 wrt PMT)
 - 3) the possibility of reading out Cerenkov light at even **higher rates (pions)**
- The main issues concerning the use of SiPM are:
 - 1) the **high dark rate**, which can be easily solved by cooling
 - 2) the **radiation damage**, which is still to be investigated in detail (concerning the expected dose and the possible hadronic shields upstream the CEDAR).
BTW we can think of regularly substituting SiPM's if damage stays below an acceptable level at least for 30 days of data-taking.
- Next steps will be test beams (during Fall 2008):
 - 1) **illumination with Cherenkov light** for measuring : **p.e. Yield** and **timing**
 - 2) exposition of samples to the K12 beam line halo for measuring the **radiation effects**



Additional information

The silicon photomultiplier

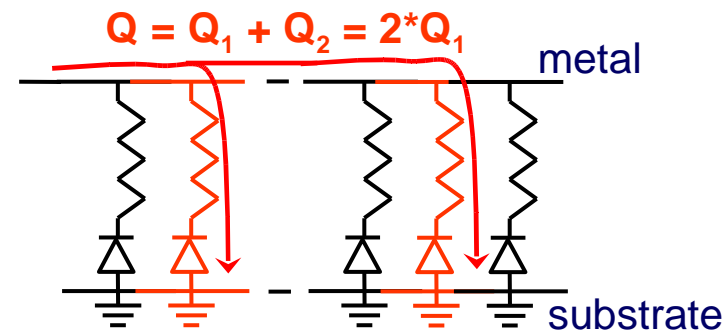
MATRIX of Geiger-Mode APD's first proposed by Golovin and Sadygov in 90ies



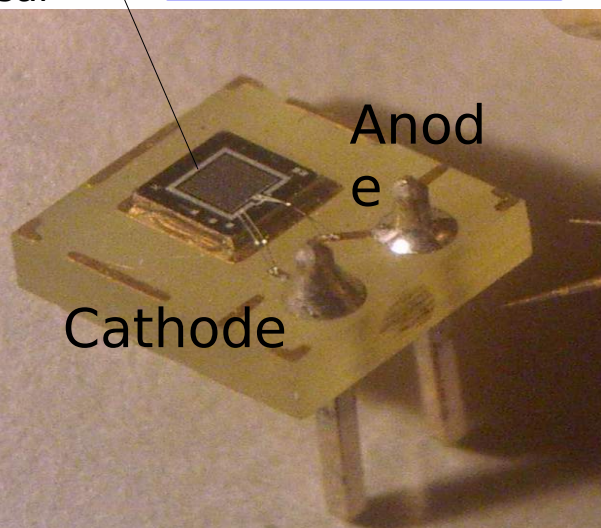
A single SiPM is segmented in tiny **micro GM-APD cells** with one **passive quenching R_Q** each and **connected in parallel**.

Each element is independent and gives the same signal when fired by a photon

Output charge is proportional to the number of triggered cells that is the number of incident photons (if efficiency = 1)



Σ digital signals = analog signal !!!

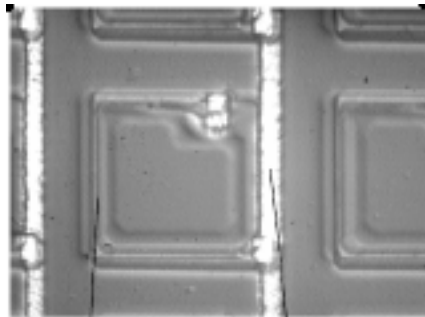


A bit of history of SiPM

Pioneering work since late 80-ies at Russian institutes

Investigations of various multi-layer silicon structures with local micro-plasma suppression effect to develop low-cost APD devices

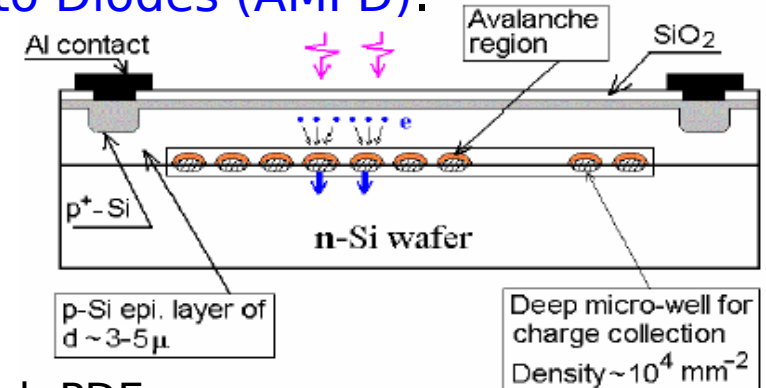
Dolgoshein - Mephi/PULSAR (Moscow) Polysilicon resistor



Si⁺ Resistor Al - conductor

- Low area efficiency
 - Standard fabrication tech.
- e.g., Dolgoshein, NIMA 563 (2006)

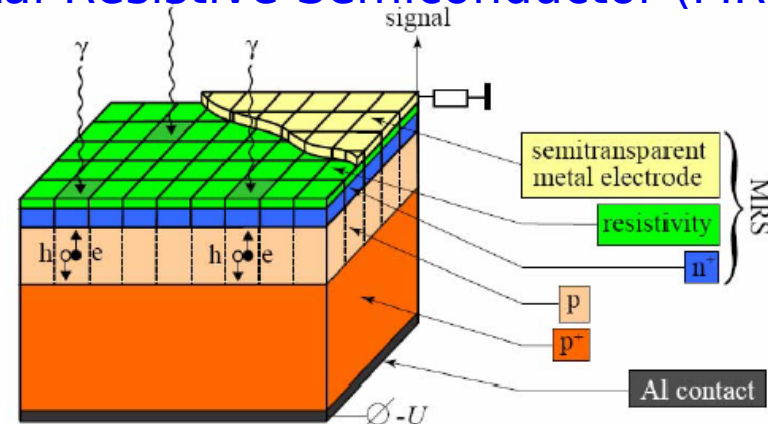
Sadygov - JINR (Dubna) Avalanche Micro-channel/pixel Photo Diodes (AMPD).



- high PDE
- very high density of microcells

Sadygov, NIMA 567 (2006)

Golovin - Obninsk/CPTA (Moscow) Metal-Resistive-Semiconductor (MRS)

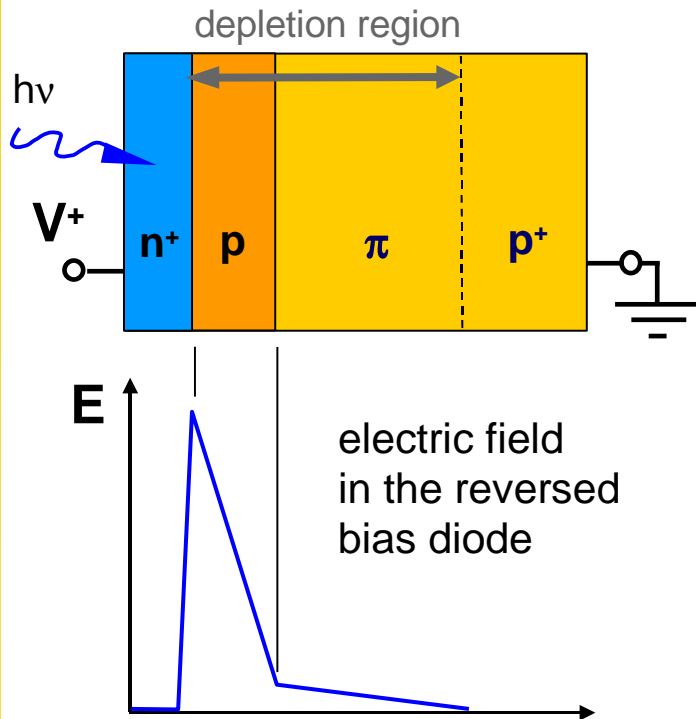


- High Area efficiency
- high density of microcells

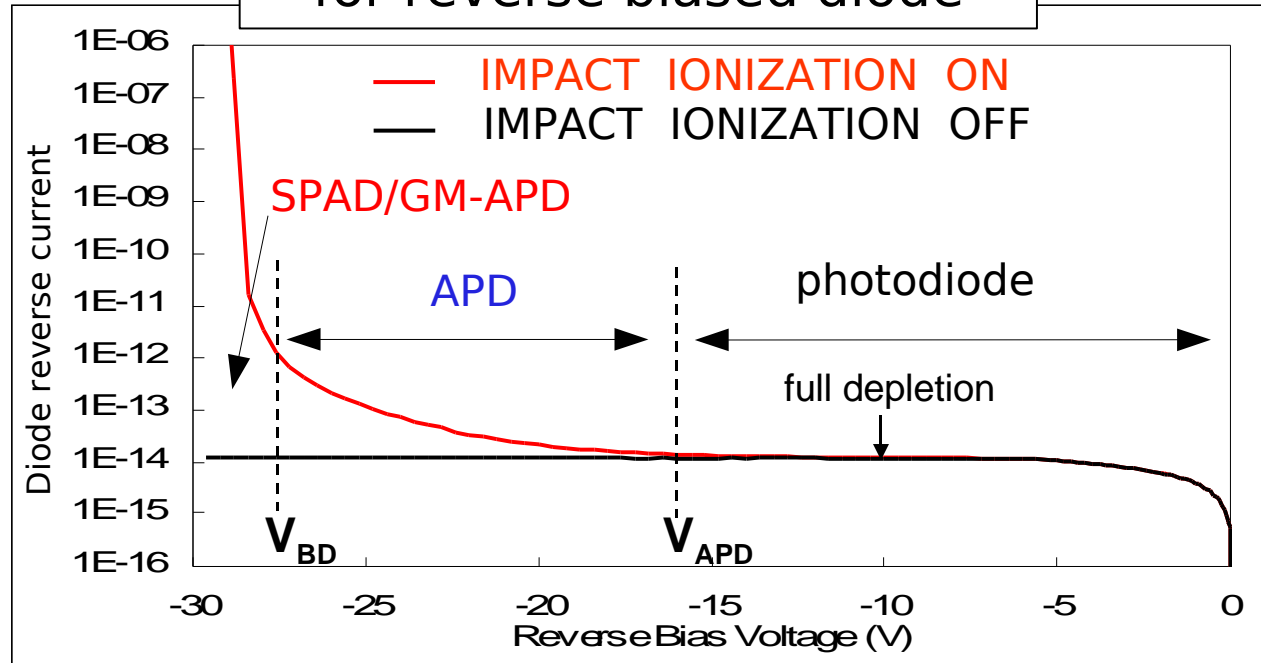
e.g., Golovin
NIMA 539 (2005)

The building block of a SiPM: SPAD/GM-APD

Reverse polarized p-n junction



Different working regimes for reverse biased diode



APD: Linear-Proportional Mode

- Bias **BELOW** V_{BD} ($V_{APD} < V < V_{BD}$)
- It's an **AMPLIFIER**
- Gain: limited < 1000 due to fluctuations
- Strong dependence on T and V_{bias}
- No single photo-electron resolution

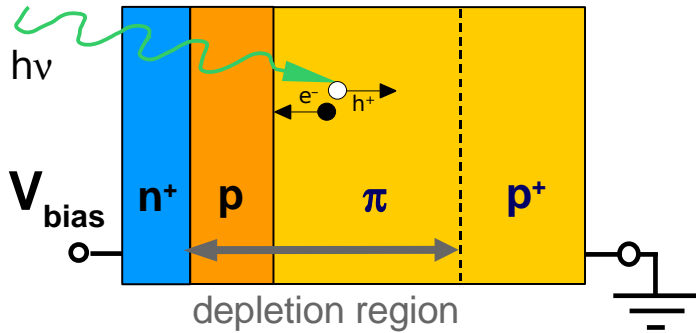
SPAD/GM-APD: Geiger Mode

- Bias **ABOVE** V_{BD} ($V - V_{BD} \sim$ a few volts)
- It's a **TRIGGER** (BINARY) device
- Gain: $\rightarrow \infty$
- Limited by dark count rate
- Single photo-electron resolution

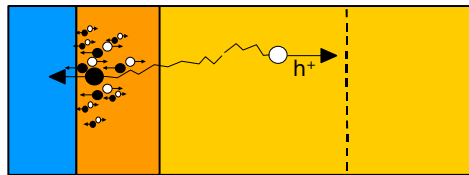
Operation principle of a GM-APD

Diode Biased ABOVE V_{BD}

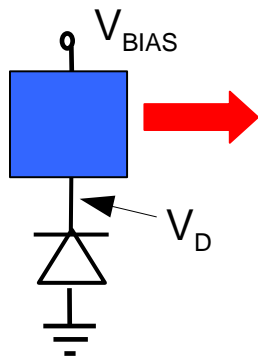
- $t=0$: carrier initiate the avalanche



- $0 < t < t_1$: avalanche spreading



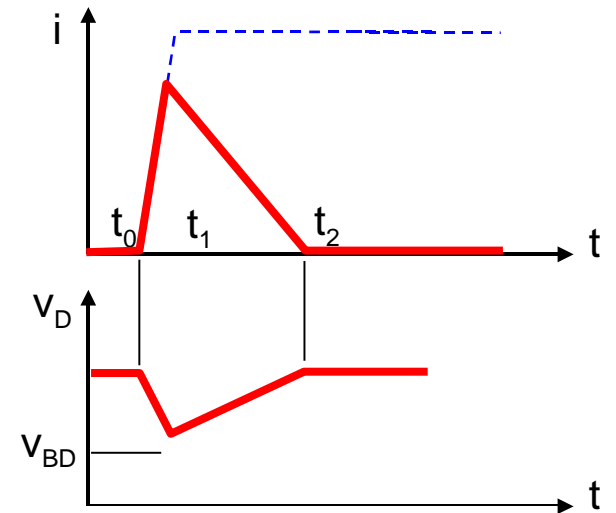
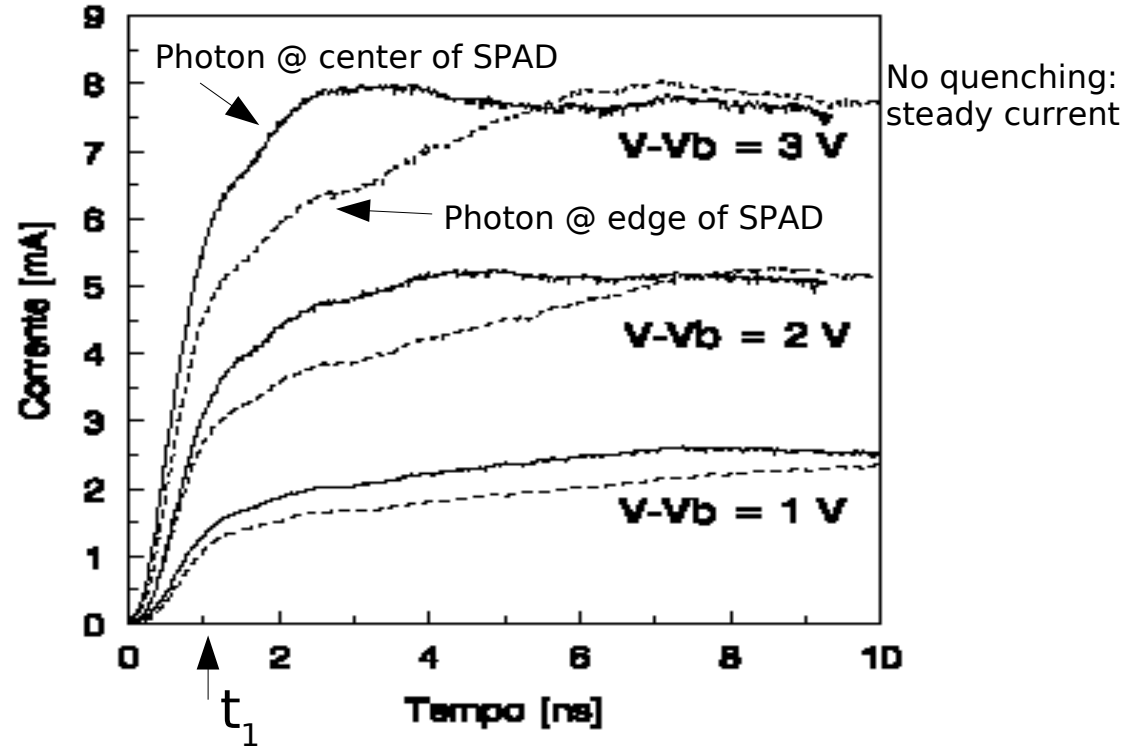
- $t_1 < t$: self-sustaining current (limited by series resistances)



To detect another photon need a **quenching mechanism**. Two solutions:

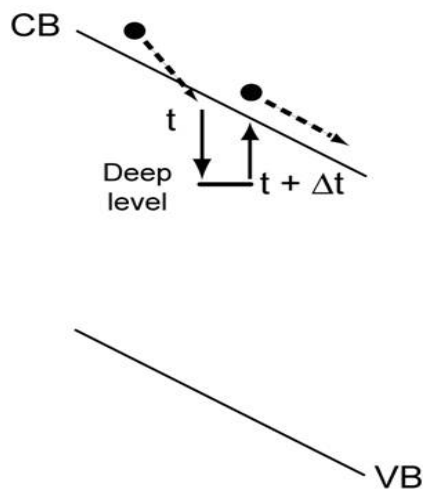
- large resistance: **passive quenching**
- analog circuit: **active quenching**

A. Spinelli Ph.D thesis (1996)



After-pulsing (delayed noise)

i.e. Carrier trapping and delayed release



$$P_{\text{after-pulse}}(t) = P_c \cdot \frac{\exp(-t/\tau)}{\tau} \cdot P_{01} \propto \Delta V^2$$

P_{01} : trigger probability

$\propto \Delta V(t)$ (over-voltage, recovery)

τ : trap lifetime

depends on trap level position

quadratic dependence on ΔV

P_c : trap capture probability

\propto carrier flux (current) during avalanche $\propto \Delta V$ (over-voltage)

$\propto N$ traps

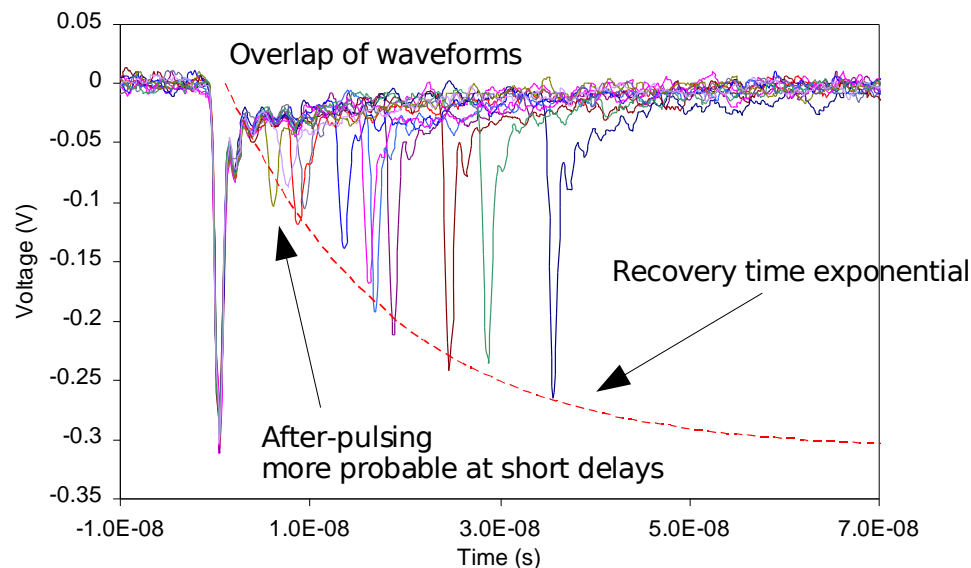
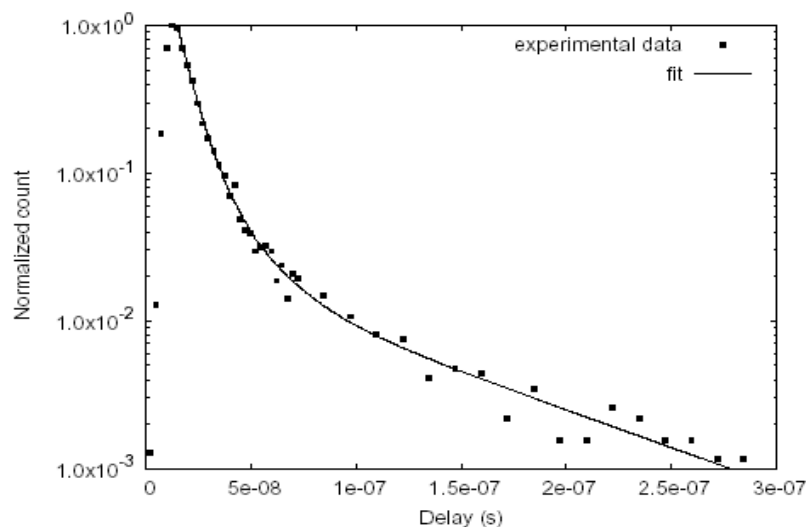


Fig. 10. Spectrum of the delay time from the primary pulse to the after-pulse. C.Piemonte et al. IEEE TNS 54 (1) (2007) 236

It can be reduced to % in a wide ΔV range

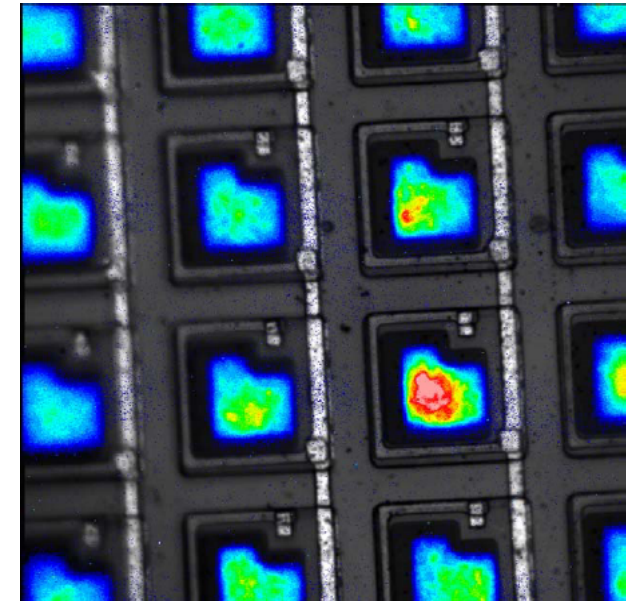
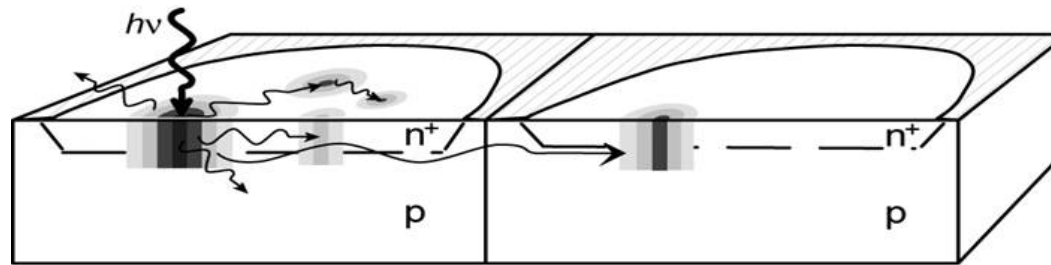
Optical cross-talk (excess noise)

Carrier luminescence (spontaneous direct relaxation in the conduction band) during the avalanche: probability $3 \cdot 10^{-5}$ per carrier (crossing the junction) to emit photons with $E > 1.14$ eV

A.Lacaita et al. IEEE TED (1993)

Photons can induce avalanches in neighboring cells.
Depends on distance between high-field regions
Quadratic dependence on over-voltage:

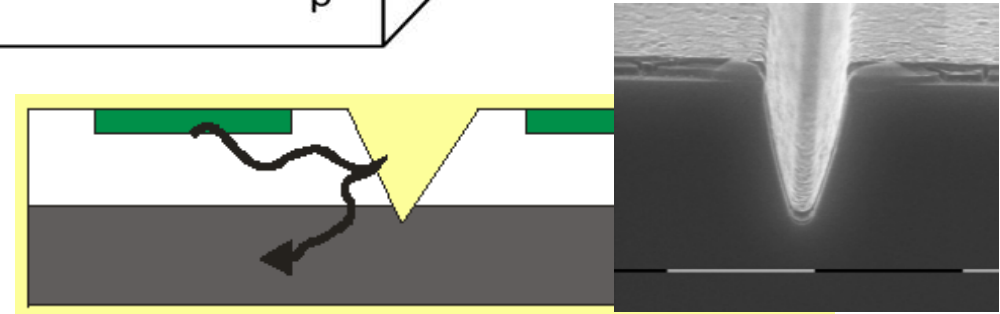
- carrier flux (current) during avalanche $\propto \Delta V$
- gain $\propto \Delta V$



N.Otte, SNIC 2006

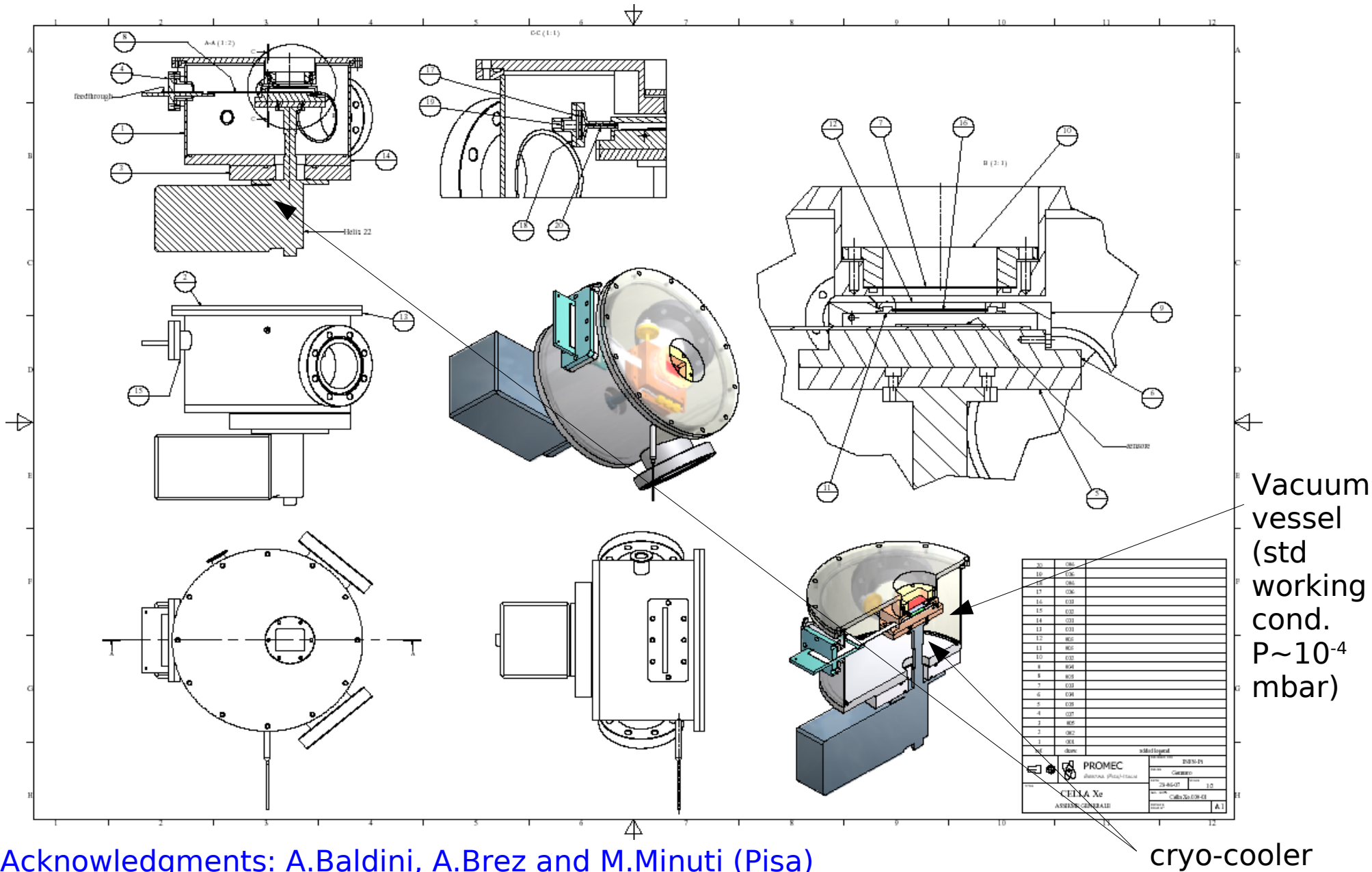
Counteract:

- **optical isolation** between cells by trenches filled with opaque material
- low over-voltage operation helps



It can be reduced below % in a wide ΔV range

Setup: vacuum vessel + cryo-cooler

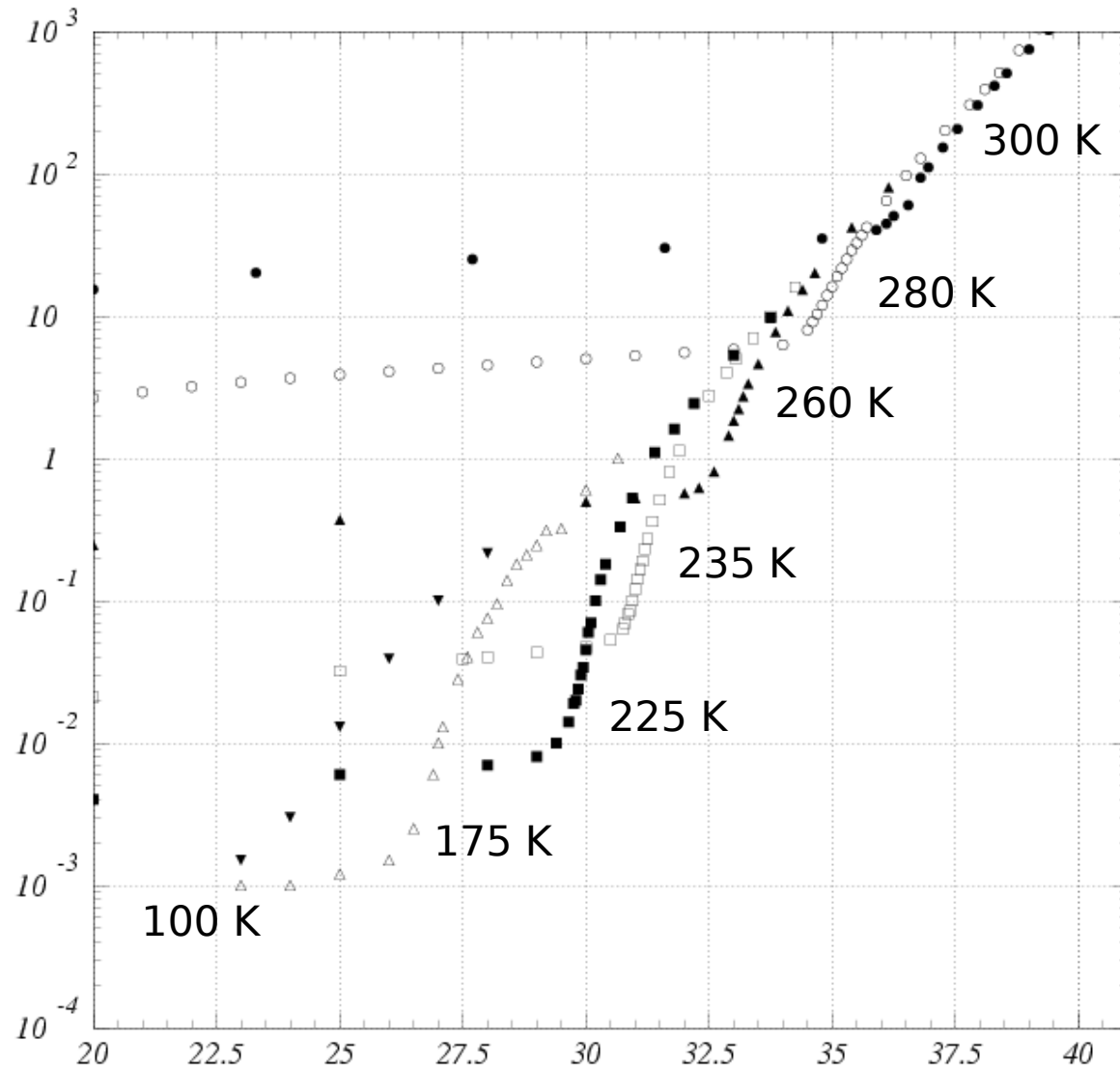


Acknowledgments: A.Baldini, A.Brez and M.Minuti (Pisa)

SiPM's are in thermal contact with a cooled Cu rod

I-V measurements at different T

SiPM type: 1mm² , fill factor 50%



T dependence: Dark rate

Dark count rate:

1. Diffusion
2. Thermal - SHR (Field Enhanced)
3. Band to Band Tunnel

$I_{reverse}$ by minority carriers: negligible at room T

Rule of thumb: x2/8K (at fixed Overvoltage)
Dominating at room T

$$I_{revers\ bias} \propto T^2 \exp\left(\frac{-E_g}{2k_B T}\right)$$

May dominate at low T
Strong dependence on Electric field

Dark rate in SPAD vs T

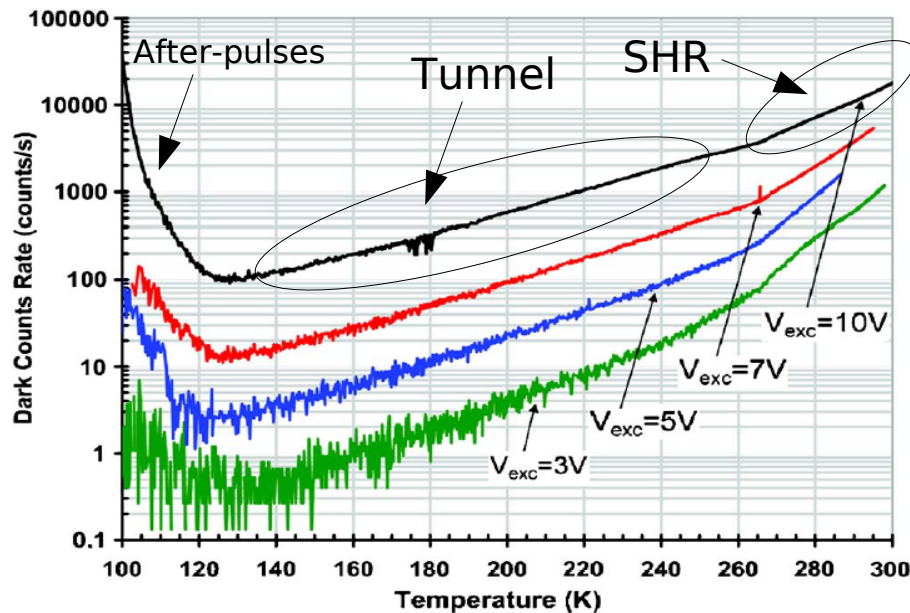
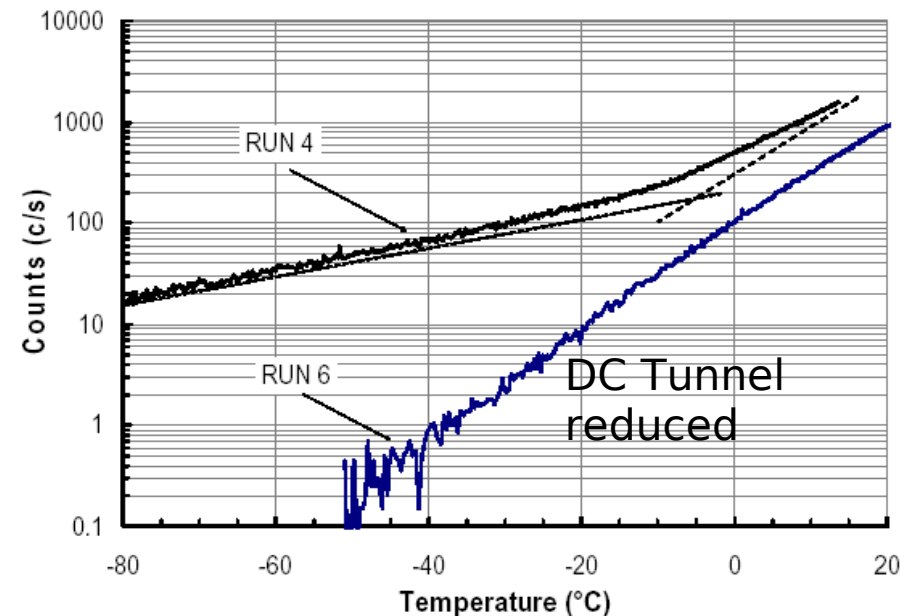


FIG. 2. (Color online) Dark counts of a thin SPAD with active area diameter of $50 \mu\text{m}$ as a function of absolute temperature for three different excess bias voltages (bottom to top: 3, 5, 7, and 10 V). Around 120 K the curves rise due to afterpulsing.

I.Rech et al, Rev.Sci.Instr. 78 (2007)

Dark rate in SPAD vs T w/ and w/o Field Engineering



I.Rech - Perugia 13/14 June 2007

Front-End Electronics

Table 1 Performance of 1GHz system

Signal to Noise ratio for 1 photo electron and PM gain 1E6
 Time resolution
 Double pulse resolution
 Analog Bandwidth
 Current consumption at $\pm 5V$
 ADC Sampling frequency
 Estimated price of the front end electronics with cables
 Readout

200
 < 20 psec rms
 5 ns
 0.4 to 200 MHz
 40 mA
 1 GHz
 25 CHF/channel
 see TELL1 board

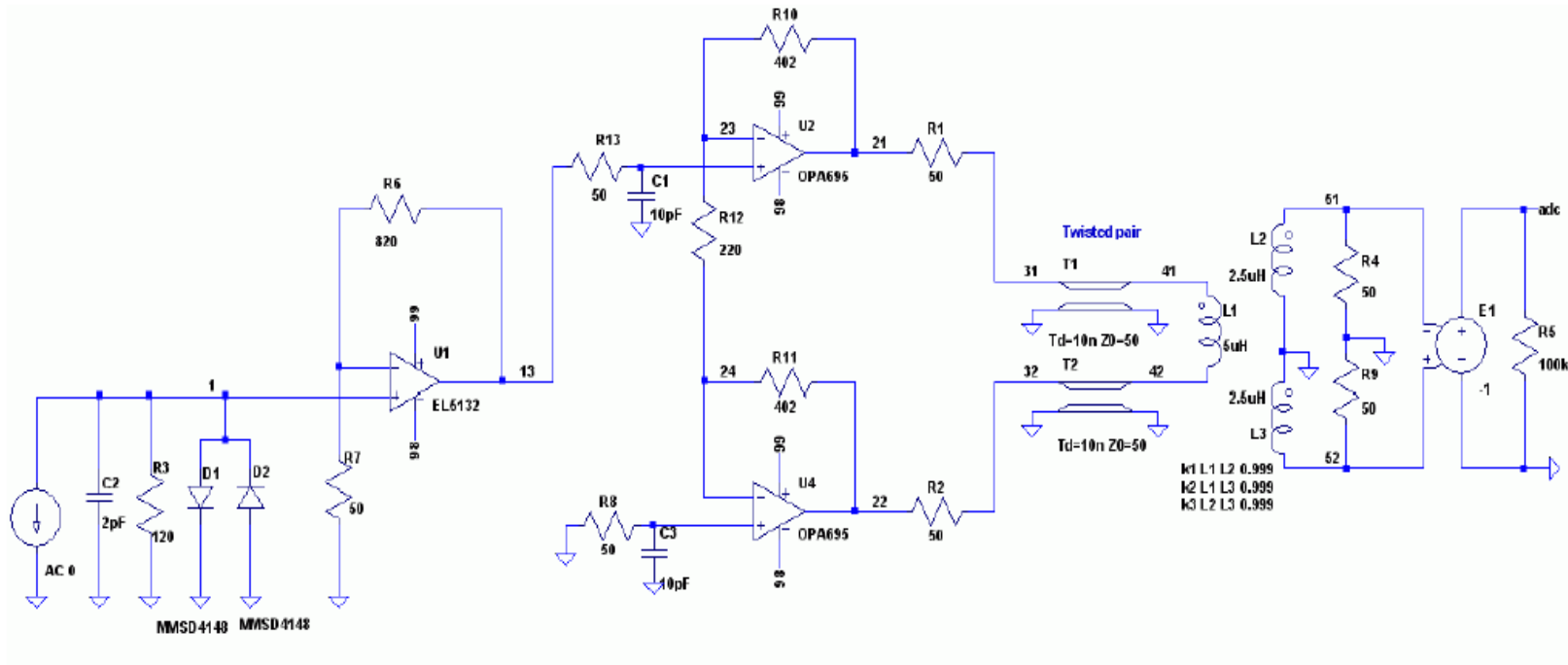


Figure 4 Schematic of front end electronics for 1GHz FADC

B.Hallgren (NA48 note 05-02, 2005)